

Oxygen loss during thermal donor formation in Czochralski silicon: New insights into oxygen diffusion mechanisms

S. A. McQuaid,^{a)} M. J. Binns,^{b)} C. A. Londos,^{c)} J. H. Tucker, A. R. Brown, and R. C. Newman

Interdisciplinary Research Centre for Semiconductor Materials, The Blackett Laboratory, Imperial College of Science, Technology and Medicine, Prince Consort Road, London SW7 2BZ, United Kingdom

(Received 5 August 1994; accepted for publication 8 November 1994)

As-grown Czochralski silicon samples with different oxygen concentrations have been heated at temperatures in the range 350–500 °C. Oxygen loss during anneals at low temperatures ($T \leq 400$ °C) is shown to follow second-order kinetics and measurements led to values of oxygen diffusivity that were larger than normal by a factor of ~ 3 , assuming the capture radius for dimer formation was 5 Å. Variations in the rate of $[O_i]$ loss during more extended anneals could be explained if oxygen diffusion was initially enhanced but tended to its normal value as the anneals progressed. Much greater initial enhancements were derived from similar measurements for samples which had been hydrogenated by a heat treatment in H_2 gas at 1300 °C for 30 min followed by a rapid quench to room temperature, and the enhancements were consistent with values derived from measurements of the relaxation of stress-induced dichroism. At higher temperatures ($T \geq 450$ °C) the measured rates of $[O_i]$ loss were less than the expected rate of O_i - O_i interaction and tended to vary with increasingly high powers of $[O_i]$. Modeling of the clustering process demonstrated that the reductions could be explained if the oxygen dimers were present in a quasiequilibrium concentration throughout the anneals. The establishment of this equilibrium appears to require that oxygen dimers diffuse much more rapidly than isolated O_i atoms. The kinetics of oxygen loss over the whole range of temperatures can then be explained if dimer clustering leads mainly to increases in concentrations of agglomerates containing large numbers (≥ 8) of oxygen atoms. It is therefore possible to account for thermal donor (TD) formation based on the formation of different sizes of oxygen clusters, although the possibility that self-interstitials are involved in TD formation is not excluded. © 1995 American Institute of Physics.

I. INTRODUCTION

As-grown Czochralski (Cz) silicon contains isolated interstitial oxygen atoms in concentrations $[O_i] \sim 10^{18} \text{ cm}^{-3}$. This is a highly supersaturated solution but it is stable because the impurities are not mobile at room temperature. Oxygen diffusion has been measured^{1–9} over the wide range of temperatures $1280 \geq T \geq 300$ °C and “normal,” i.e., unenhanced, values (Fig. 1) are described by $D_{\text{oxy}} = 0.13 \exp(-2.53 \text{ eV/kT}) \text{ cm}^2 \text{ s}^{-1}$. If the temperature is raised above ~ 350 °C, the diffusion coefficient of O_i atoms D_{oxy} becomes sufficiently large for long-range migration to occur and there is then a measurable loss of these atoms from solution due to the formation of oxygen clusters.^{10,11}

Heat treatments at high temperatures ($T \geq 650$ °C) lead to the growth of SiO_2 precipitates which can be monitored by transmission electron microscopy (TEM),^{12–14} defect etching, and small-angle neutron scattering (SANS).^{15,16} Measurements demonstrated that the number density of precipitates N was relatively independent of anneal time once the initial transient associated with the nucleation stage had occurred.¹⁷ The observed tendency of N to decrease slowly

after long anneals was explained in terms of Ostwald ripening, implying a dynamical equilibrium between the capture of O_i atoms from solution and their dissolution from precipitates. Quasiequilibrium values of $N = 6 \times 10^3 \exp(3.0 \text{ eV/kT}) \text{ cm}^{-3}$ were determined in material heated in argon at various anneal temperatures¹⁶ and the effective diffusion coefficient of oxygen atoms could then be deduced from measurements of the loss of $[O_i]$ during isothermal anneals using the kinetic equations of Ham.¹⁸ The values of D_{oxy} deduced in this way^{12,16,17} corresponded to normal oxygen diffusion (Fig. 2) in agreement with an analysis of TEM results.¹³ Normal oxygen diffusion was therefore shown to be the rate-limiting step for precipitation even though self-interstitial generation must have occurred at the surfaces of the SiO_2 particles followed by diffusion into the surrounding matrix in order to accommodate the local increase in volume.^{19–23}

Following anneals at lower temperatures ($485 \leq T \leq 650$ °C) TEM measurements revealed unidentified “black dot” contrast together with long ribbonlike defects (RLD). On the basis of optical-diffraction patterns obtained from TEM direct lattice images these defects were attributed to coesite,^{24,25} a high-pressure phase of silica. The formation of oxygen clusters as large as the RLDs at 485 °C would have required the oxygen diffusivity to have been enhanced²⁶ by a factor of 10^4 (Fig. 2); however, observation of TEM contrast does not necessarily imply that the defect involves atoms other than silicon. Subsequently the use of the electron-energy-loss technique provided no evidence for the presence

^{a)}Present address: Departamento de Ingenieria Electronica, Universidad Politecnica de Madrid, ETSIT, Ciudad Universitaria s/n, 28040 Madrid, Spain.

^{b)}Present address: MEMC Electronic Materials, Inc., 501 Pearl Dr., P.O. Box 8, St. Peters, MO 63376.

^{c)}Permanent address: Solid State Physics Section, Department of Physics, Panepistimiopolis, GR 157 84-Zografos, Athens, Greece.

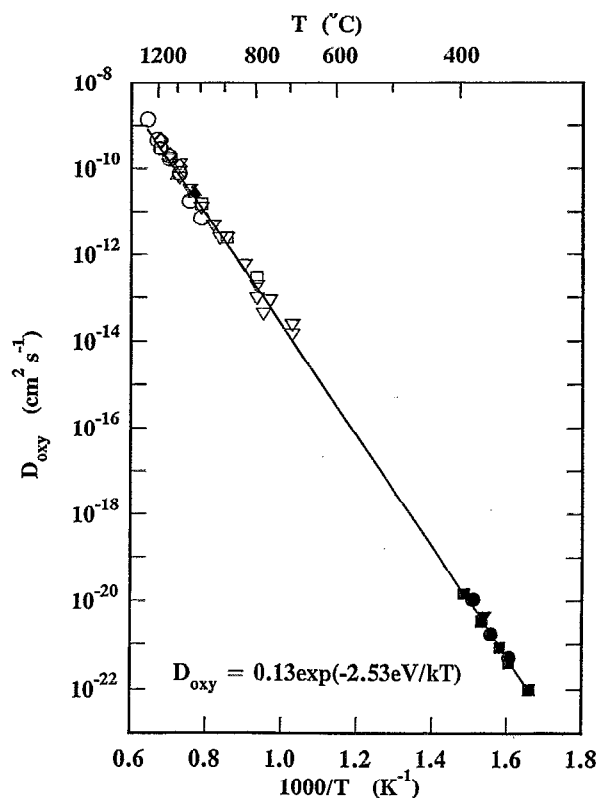


FIG. 1. Measured values of normal oxygen diffusion (Refs. 1–9) together with a line fitted to all the data given by $D_{\text{ox}} = 0.13 \exp(-2.53 \text{ eV}/kT)$ $\text{cm}^2 \text{ s}^{-1}$.

of high concentrations of oxygen atoms in the RLDs which were instead attributed to hexagonal silicon nucleated by the agglomeration of self-interstitials.²⁷ These Si interstitials were assumed to have been generated during formation of much smaller oxygen clusters which might have produced the black dot contrast. In a more recent TEM study the attribution of RLDs to hexagonal silicon has been questioned,²⁸ but no alternative structure was suggested. Nevertheless, oxygen has been detected²⁹ in RLDs formed during an anneal at 635 °C but the oxygen/silicon ratio (~6%) was too low to be consistent with the assignment to SiO_2 . In fact, the levels of oxygen detected can be explained by the precipitation of oxygen with normal D_{ox} on to a structure otherwise involving only self-interstitials. Irrespective of this uncertainty, oxygen clusters as large as RLDs should have been detected by SANS, contrary to experimental results.^{17,30,31} In summary, although large defects have been observed, they do not appear to correspond to oxygen clusters and the TEM data cannot be considered to provide reliable evidence for enhanced oxygen diffusion. Secondary-ion-mass-spectrometry (SIMS) measurements of oxygen out-diffusion^{32,33} at similar temperatures have lead to anomalously large estimates of D_{ox} (Fig. 2); however, these measurements can only be made within a short distance (~10 μm) of the surface where an in-diffusing impurity or defect might cause a local enhancement, while normal oxygen diffusion may occur in the bulk of the sample in which such

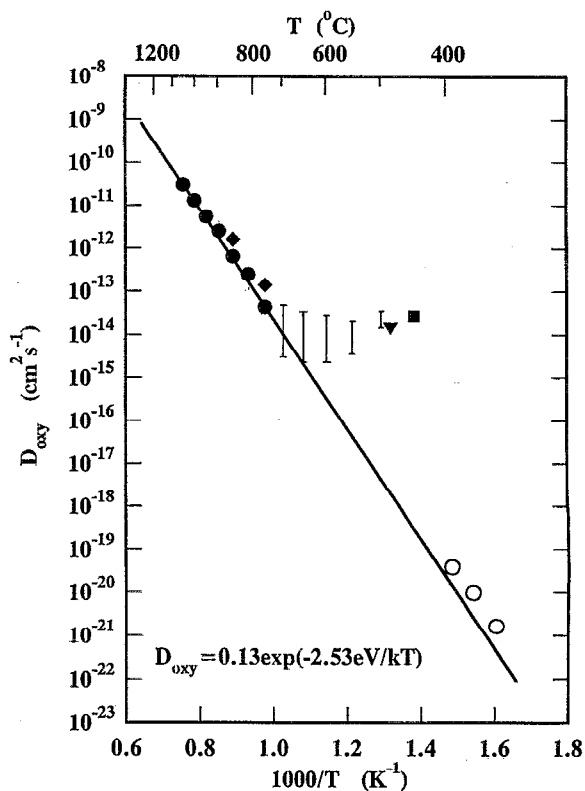


FIG. 2. Estimates of oxygen diffusion derived from analyses of oxygen loss (Ref. 15) (\bullet), SiO_2 precipitate growth (Ref. 13) (\blacklozenge), and kinetics of RLD formation (Ref. 19) (\blacktriangledown) together with values implied by out-diffusion measurements by SIMS (Ref. 28) (vertical lines) and TD profiling (Ref. 26) (\blacksquare). Analysis of the present $[\text{O}_i]$ -loss measurements, assuming a value of $r_c = 5$ Å, for as-grown material annealed at $T \leq 400$ °C (\circ) are also shown. The line represents that fitted to measurements of D_{ox} (Fig. 1).

point defects are likely to be absent. In fact, significantly enhanced out-diffusion at the higher temperatures of 750, 1000, and 1200 °C has also been reported,^{34–36} although there is no doubt that oxygen diffusion to precipitates is normal at these temperatures, as discussed above.

At the lowest temperatures ($T \leq 500$ °C), oxygen aggregation leads to the formation of thermal donor (TD) defects. Early work by Kaiser, Frisch, and Reiss *et al.*³⁷ revealed a dependency of the initial rate of donor formation $d[\text{TD}]/dt$ on the fourth power of the oxygen concentration during anneals at 450 °C. Kinetic arguments led to the conclusion that TD defects contained predominantly O_4 clusters and this assignment has been generally accepted and widely quoted since then. Subsequently, it was noticed³⁸ that the formation of such four atom clusters would require D_{ox} to be enhanced by a factor of 10. In fact, a structural model of TDs involving clusters of five or more O_i atoms was then shown to account for a wide variety of the experimentally observed properties of TD defects¹⁹ and this model required values of D_{ox} which were more than two orders of magnitude larger than normal. Spreading resistance profiles³⁹ of material heated at 450 °C revealed a depletion of $[\text{TD}]$ close to the surface. If oxygen out-diffusion were responsible, an enhancement of D_{ox} by a factor greater than 10^4 would again be implied (Fig. 2); however, SIMS measurements⁴⁰ revealed no evidence for such

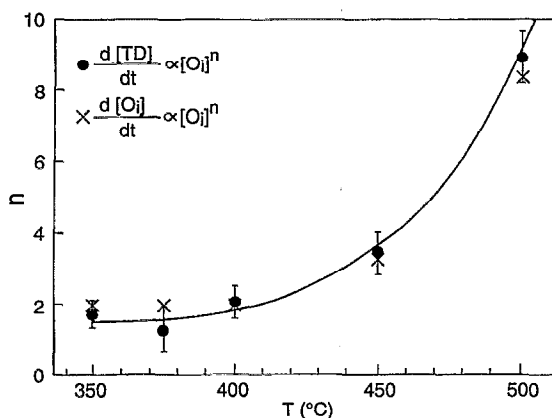


FIG. 3. The power dependency n of the initial rates of thermal donor formation (●) and loss of $[O_i]$ from solution (×) on the initial value of $[O_i]$ as functions of anneal temperature.

enhanced out-diffusion of oxygen at 450 °C and the origin for the depletion of [TD] close to the surface remains unknown. Although TD defects have been studied over a period of almost 40 years, neither their structure nor even the number of oxygen atoms present in each donor center is known.

Recently⁴¹ we measured the initial rates of TD formation for samples with different values of $[O_i]$ for a range of anneal temperatures ($350 \leq T \leq 500$ °C). The dependence of the rates on the exponent n of the grown-in oxygen concentration (i.e., $[O_i]^n$) was determined and our results at 450 °C reproduced the value of $n \sim 4$ found by Kaiser and co-workers; however, the exponent n was found to depend on anneal temperature, approaching 9 at 500 °C and tending asymptotically to ~ 2 for $T \leq 400$ °C (Fig. 3). Applying the kinetic arguments of Kaiser and co-workers to the results at the lowest temperatures would then imply that TD centers contain only two oxygen atoms and there would no longer be a requirement for D_{oxy} to be enhanced.

An extrapolation of the high-temperature ($1050 \geq T \geq 650$ °C) data³¹ for N would imply that mainly O_2 dimers would be produced at $T \sim 480$ °C and lower temperatures, consistent with the findings outlined above. An analysis of oxygen loss based on second-order kinetics, assuming that O_2 dimers did not dissociate, led to normal values of D_{oxy} for samples heated at 420 or 450 °C,^{11,17} for what was considered to be a reasonable choice of $r_c = 10$ Å for the capture radius associated with dimer formation. The magnitude of the rate of oxygen loss was therefore shown to be consistent with dimer formation being the rate-limiting step in the aggregation process, and oxygen diffusivity did not appear to have been enhanced. Since the oxygen aggregates formed during anneals at temperatures below 650 °C could not be detected directly, values of N are unknown and D_{oxy} can no longer be determined from oxygen-loss data without invoking a model to describe the aggregation process.

Notwithstanding the success of this simple dimer formation model at lower temperatures, problems became apparent after its application to further measurements. First, the analysis of measurements made on samples annealed at 500 °C led to a value of D_{oxy} that was a factor of 4.6 too small.¹⁷ This

result was attributed qualitatively to the increasing importance of dimer dissociation as the temperature was increased above 450 °C. Second, the values of D_{oxy} derived from measurements on different samples annealed at 450 °C increased linearly with the grown-in oxygen concentration.^{42,43} This result is not physically meaningful, and indicates that one or more important processes had not been taken into account in the simple dimer formation model. Third, measurements of oxygen loss in as-grown material annealed at the lowest temperatures studied (~ 350 °C) implied that D_{oxy} was enhanced by a factor of up to 10.^{44,45}

Not only was dimer dissociation neglected in the simple dimer formation model but the possibility that O_2 dimers might diffuse more rapidly as an entity than O_i atoms was also ignored. This possibility was first proposed by Gösele and Tan⁴⁶ who suggested that O_2 dimers were “gaslike molecules” that could migrate easily through the silicon lattice and that pairs of such molecules could combine to form O_4 clusters to explain TD formation according to the observations of Kaiser and co-workers.³⁷ Subsequent *ab initio* calculations^{47–50} indicated that there is a small binding energy (0.1–1.0 eV) between two adjacent O_i atoms and that these dimers have a lower activation energy for diffusion (~ 1.4 eV) than single O_i atoms. Measurements by SIMS of enhanced out-diffusion of oxygen at $T \geq 500$ °C (Fig. 2) were considered to provide evidence in support of this model.⁴⁰ These measurements led to values of D_{oxy} that were close to a value deduced from TEM observations of RLDs assuming that they consisted of coesite; however, the values derived from SIMS measurements did not vary systematically with the initial oxygen content of different samples as might have been expected and there is no evidence for high concentrations of oxygen in RLDs (see above). In conclusion, these experiments are not considered to provide conclusive evidence that oxygen dimers diffuse more rapidly than O_i atoms.

In view of the discrepancies in the literature regarding oxygen diffusion mechanisms, we have measured the rates of loss of $[O_i]$ from solution and the concomitant rates of formation of TD defects in a range of crystals during anneals at temperatures in the range $350 \leq T \leq 500$ °C which are described in Sec. II. The dependence of the rate of $[O_i]$ loss on initial oxygen concentration demonstrates that this process follows second-order kinetics at low temperatures ($T \leq 400$ °C). The values of D_{oxy} derived from an analysis of these measurements depend inversely on the value chosen for the capture radius associated with dimer formation r_c . In principle, r_c has a minimum value of ~ 2 Å, corresponding to the separation of adjacent bond-centered sites, but is not expected to exceed ~ 10 Å. As the value is not known we assumed a value of $r_c = 5$ Å to conform with that chosen by other workers.⁴² Values of D_{oxy} so deduced are shown to be larger than normal by a factor of ~ 3 and support for the small enhancements is provided by variations in the rate of $[O_i]$ loss during extended anneals. Further measurements relating to samples that had been preheated at 1300 °C in hydrogen gas and then quenched to room temperature are presented in Sec. III. Values of D_{oxy} derived in the same way for

TABLE I. Initial interstitial oxygen, substitutional carbon, and boron concentrations in the six crystals used in the present study.

Crystal	$[O_i] (\times 10^{17} \text{ cm}^{-3})$	$[C_s] (\times 10^{16} \text{ cm}^{-3})$	$[B] (\times 10^{14} \text{ cm}^{-3})$	Supplier
A	15.0	3	Undoped	Wacker Chemitronic
B	11.6	<1	2	MEMC
C	11.0	<1	4	MEMC
D	9.33	<1	5	MEMC
E	8.25	<1	<1	MEMC
F	9.60	<1	1	Philips

these samples were greater by factors of ~ 100 compared with those for samples that had not been pretreated. These enhancements are compatible with measurements of enhanced rates of relaxation of stress-induced dichroism in similarly treated samples.^{51,52} It is then demonstrated by kinetic modeling (Sec. IV) that $[O_i]$ -loss measurements at higher temperatures ($T \geq 450^\circ\text{C}$) cannot be explained in terms of serial reactions involving only diffusing O_i atoms. By assuming that oxygen dimers diffused much more rapidly than isolated O_i atoms, experimental observations could be attributed to the increasing significance of their dissociation at temperatures higher than 400°C .

II. EFFECT OF VARIATION OF OXYGEN CONCENTRATION

Samples were cut ($\sim 10 \times 10 \times 1.5 \text{ mm}^3$) from Cz crystals A–E (Table I) that had not been subjected to any postgrowth heat treatment. Sets of specimens were polished and annealed isothermally in air at 350, 375, 400, 450, and 500°C . The absorption coefficient α of the $9 \mu\text{m}$ infrared (IR)-absorption band was measured at room temperature at each stage of the anneal using a Perkin-Elmer PE983 double-beam dispersive spectrometer. Values of $[O_i]$ were determined using the ASTM procedure⁵³ in conjunction with the calibration of Baghdadi *et al.*⁵⁴ for which $\alpha = 1 \text{ cm}^{-1}$ corresponds to $[O_i] = 3.14 \times 10^{17} \text{ cm}^{-3}$. Resistivity measurements were made using the four-point-probe technique and applying the appropriate correction factors to account for the finite sample thickness.⁵⁵ Values of $[TD]$ were deduced using the previously reported calibration.⁵⁶

As discussed above, in the low-temperature regime ($T < 500^\circ\text{C}$) the rate of loss of oxygen from solution should be related to trapping of diffusing O_i atoms by other such atoms resulting in the formation of an O_2 dimer described by



Assuming the dissociation rate of the dimers is negligible relative to the forward reaction rate, the kinetics of $[O_i]$ loss would be controlled solely by the interaction rate of two randomly diffusing O_i atoms,

$$\frac{d[O_i]_t}{dt} \sim -8\pi r_c D_{\text{oxy}} [O_i]^2, \quad (2)$$

where r_c is the capture radius associated with dimer formation. Integrating this expression leads to the relation

$$1/[O_i]_t = 1/[O_i]_0 + 8\pi r_c D_{\text{oxy}} t, \quad (3)$$

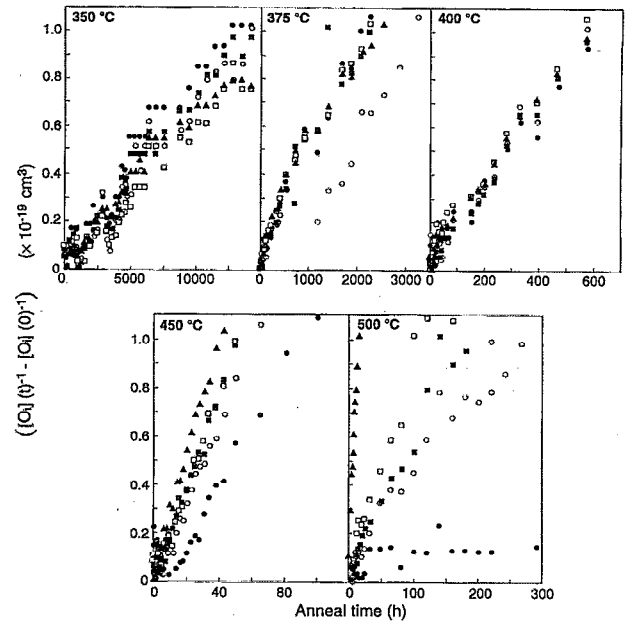


FIG. 4. Loss of the first 10% of $[O_i]$ during anneals at the indicated temperatures, plotted in the form $([O_i]^{-1})_t$ and normalized by subtracting the inverse of the initial concentrations in the different samples prepared from crystals (\blacktriangle) A, (\square) B, (\blacksquare) C, (\circ) D, and (\bullet) E. The initial concentration was estimated by the extrapolation to $t=0$ of a least-squares fit to the data for each sample.

where $[O_i]_0$ represents the concentration of isolated oxygen atoms prior to the anneals. Plots of $[O_i]^{-1}$ versus time are therefore expected to be linear with a gradient equal to $8\pi r_c D_{\text{oxy}}$, irrespective of the value of $[O_i]_0$ which should only modify the offset constant.

The experimental results representing the loss of the first 10% of $[O_i]_0$ are shown in Fig. 4. The gradients of lines fitted to the data did not depend on $[O_i]_0$ for anneals at low temperatures ($T \leq 400^\circ\text{C}$). Values of D_{oxy} derived from these slopes using Eq. (3) and assuming a value of $r_c = 5 \text{ \AA}$ were independent of $[O_i]_0$ (Fig. 5), as expected for second-order kinetics. After longer anneal times the slope of the data tended to decrease (Fig. 6). Reductions in the rate of $[O_i]$ loss are expected when the dissociation of the clusters formed during the anneal becomes significant. Since the concentration of such clusters should increase with anneal time, the reductions would then become increasingly more apparent; however, the form of the variation did not vary significantly with $[O_i]_0$ in the different samples and there was no tendency to approach an asymptotic concentration after long anneal times. An alternative explanation would follow if D_{oxy} was enhanced initially but then decreased toward its normal value with increasing anneal time.

At 450°C values of D_{oxy} (Fig. 5) estimated from the initial gradient of the plots of $[O_i]^{-1}$ against anneal time increased linearly with increasing $[O_i]_0$ in the different samples, in agreement with previous observations.^{42,43} At 500°C the rate of loss of $[O_i]$ varied with $[O_i]^8$ (Fig. 3), corresponding to an apparent variation of D_{oxy} with $[O_i]^6$ [Eq. (2) and Fig. 5]. This dependence is not physically mean-

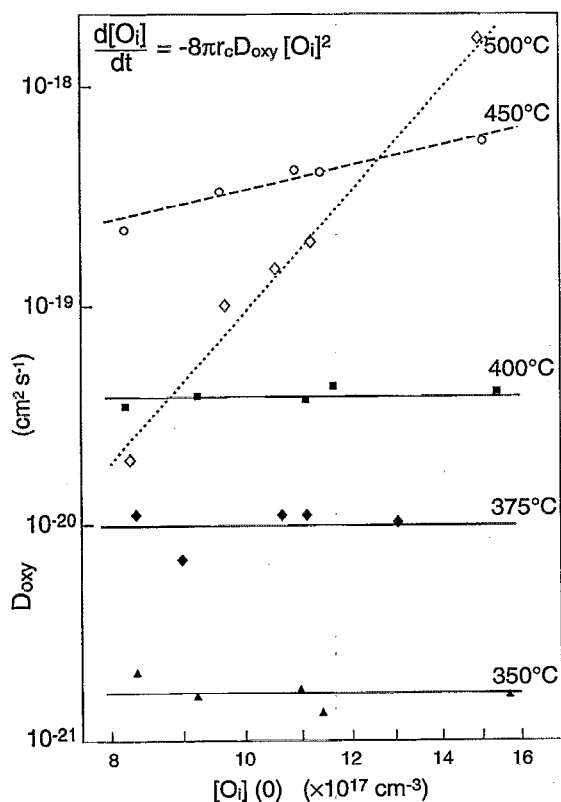


FIG. 5. Values of D_{oxy} derived from the gradients of the lines fitted to the first 10% of $[\text{O}_i]$ loss (Fig. 4) for as-grown samples annealed at (▲) 350, (◆) 375, (■) 400, (○) 450, and (◇) 500 °C as a function of the initial value of $[\text{O}_i]$.

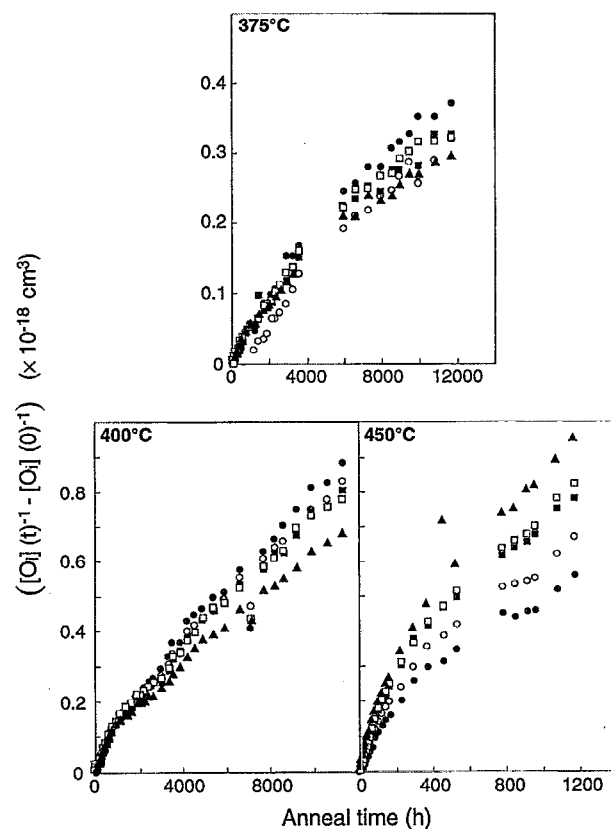


FIG. 6. Loss of $[\text{O}_i]$ during extended anneals at the indicated temperatures, plotted in the form $([\text{O}_i]^{-1})_{(t)}$ and normalized by subtracting the inverse of the initial concentrations in the different samples.

ingful (see Sec. I), indicating that some other process or processes became significant at these higher temperatures. This shortcoming is revealed by a comparison of the implied values of D_{oxy} with those expected for normal diffusion (Fig. 7). While the values of D_{oxy} appear to be larger than normal by a factor of ~ 3 at the lower temperatures ($T \leq 400$ °C), independent of the value of $[\text{O}_i]_{(0)}$, the corresponding values at 450 °C are close to normal and those derived from the 500 °C data are lower than normal, particularly for samples with a low initial oxygen concentration. By implication, the rate of $[\text{O}_i]$ loss was less than expected at the higher temperatures if a stable O_2 dimer had been formed for every O_i - O_i interaction. These effects indicate that the rate of a reverse dissociative reaction must have become increasingly significant relative to that of O_i - O_i interaction as the temperature was increased ($T \geq 450$ °C). This is apparently in contradiction to the conclusions based on the form of plots of $([\text{O}_i]^{-1})_{(t)}$, which did not change significantly with anneal temperature over the whole range investigated (Fig. 8). This problem is considered further in Sec. IV.

We next consider the measurements of thermal donor concentration made for the same set of samples. At temperatures below 400 °C the rate of TD formation, estimated for values of $[\text{TD}]$ up to $\sim 5 \times 10^{15} \text{ cm}^{-3}$, varied with $[\text{O}_i]^2$ (Fig. 3), as reported previously.⁴¹ This result indicates that oxygen dimerization was not only the rate-limiting step for the loss of $[\text{O}_i]$ from solution but also for the formation of TDs.

Support for the observation that the rates of both processes were controlled by the same reaction step is provided by consideration of the ratio of oxygen loss $\Delta[\text{O}_i]$ relative to the concentration of TDs formed $\Delta[\text{TD}]$. The ratio (~ 10) which could only be determined after significant $[\text{O}_i]$ loss ($> 1 \times 10^{16} \text{ cm}^{-3}$) was almost constant during the anneals until a maximum value of $[\text{TD}]$ was established (Fig. 9). In other words, the rate of TD formation decreased during long anneals, corresponding to the variations in the rate of $[\text{O}_i]$ loss already described. The ratio did not vary significantly with either $[\text{O}_i]_{(0)}$ or anneal temperature (Fig. 10) so the increasing dependence of $d[\text{O}_i]/dt$ on $[\text{O}_i]_{(0)}$ at higher temperatures was correlated with that for TD formation (Fig. 3). The dissociative reaction responsible for the reduced rates of $[\text{O}_i]$ loss at high temperatures ($T = 400$ °C) was therefore shown to lead to corresponding reductions in the rates of TD formation.

In summary, the stable dimer model describes the $[\text{O}_i]$ -loss process adequately at low temperatures ($T \leq 400$ °C) but D_{oxy} appeared to be larger than normal by a factor of ~ 3 . The slopes of graphs of $([\text{O}_i]^{-1})_{(t)}$ decreased by a similar factor after long anneals which could be explained if D_{oxy} was initially enhanced and subsequently decreased toward its normal value. It is therefore necessary to propose a mechanism for such an enhancement process. A preheat treatment of a sample in hydrogen gas is known to

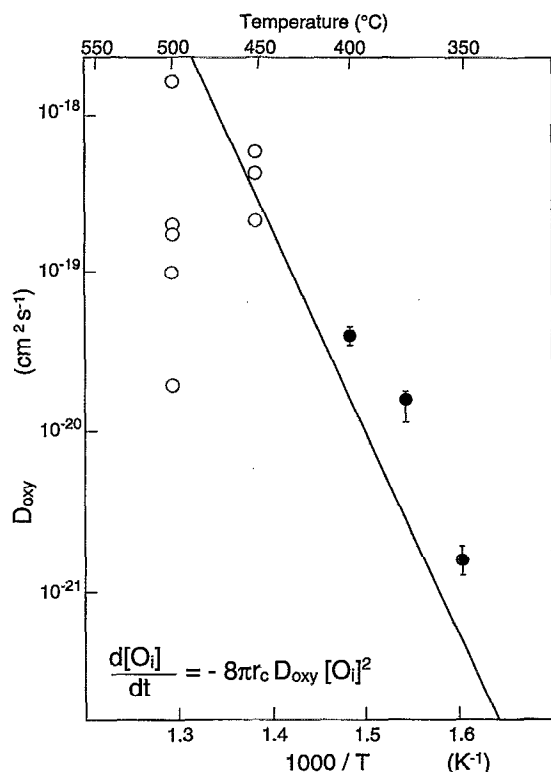


FIG. 7. An Arrhenius plot of the average values of D_{oxy} derived from the gradients of graphs of $([O_i]^{-1})_{(t)}$ for samples prepared from crystals A–E annealed at $T \leq 400^{\circ}\text{C}$ (●) and the apparent values derived in the same way from the data for the different samples annealed at $T \geq 450^{\circ}\text{C}$ (○). The line represents an extrapolation of normal values of D_{oxy} (Fig. 1).

lead to very large enhancements of the rate of single diffusion jumps of O_i atoms but there is no systematic published data for enhanced long-range oxygen diffusion in such material at temperatures in the range $500 \geq T \geq 350^{\circ}\text{C}$. We now show that this process does occur, indicating that the slightly enhanced oxygen diffusion in as-grown material may be explained by the presence of a small concentration of rapidly diffusing hydrogen.

III. EFFECT OF A PRIOR HEAT TREATMENT IN HYDROGEN

The rate of oxygen loss from solution was greatly enhanced at low temperatures in samples annealed in a hydrogen plasma rather than in air and the presence of hydrogen in the plasma was essential for the enhancement process to occur. Possible mechanisms have been discussed elsewhere.^{30,43,44,57–59} Values of enhanced D_{oxy} could not be derived from measurements of the rate of relaxation of stress-induced dichroism ($275 \leq T \leq 350^{\circ}\text{C}$) because the process appeared to be controlled by the in-diffusion of hydrogen so that the enhancement first occurred in a region close to the sample surface and the depth of this zone increased up to several millimeters with heating time;⁵⁹ however, enhanced rates of oxygen diffusion jumps have been measured for samples that had been preheated in hydrogen gas at temperatures above 600°C and then quenched to room temperature

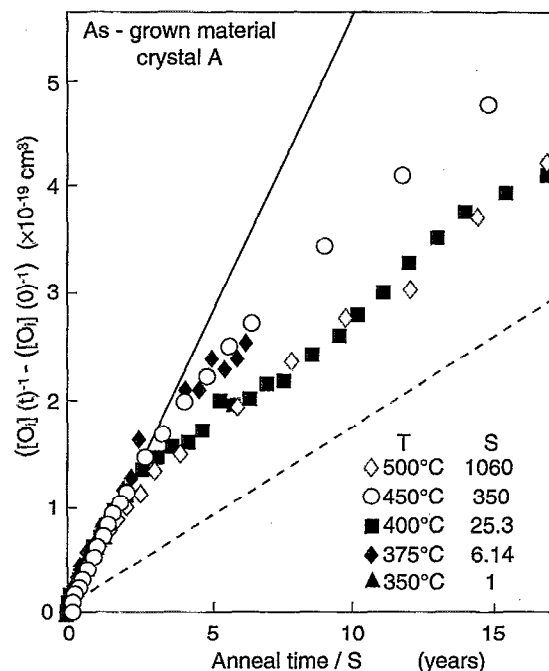


FIG. 8. The oxygen-loss data plotted in the form $([O_i]^{-1})_{(t)}$ for as-grown samples prepared from crystal A annealed at (▲) 350, (◆) 375, (■) 400, (○) 450, and (◇) 500 $^{\circ}\text{C}$ as functions of anneal time divided by a scaling factor S chosen so that the initial gradient was the same as that at 350 $^{\circ}\text{C}$ (solid line). The gradient of the dashed line is $1/3$ that of the solid line and represents the expected gradient for normal D_{oxy} .

(Fig. 11).^{51,52} The presence of hydrogen (deuterium) in material treated in this way has been demonstrated directly by SIMS measurements^{60,61} and by observation of H-B pairs in material containing $[B] \sim 10^{17} \text{ cm}^{-3}$.^{51,60–63} The concentration of hydrogen and the enhancement of the oxygen diffusion process were uniform throughout the thickness of the samples. The scatter in the measurements (Fig. 11) is relatively large and the reason is not understood. Samples had been quenched from temperatures of 800, 900, or 1250 $^{\circ}\text{C}$ but there was no systematic correlation with the resulting value of D_{oxy} . It should be recalled that if the enhancement were due to the transient interaction of highly mobile H atoms with O_i atoms, as proposed elsewhere,^{64,65} the enhancement would depend on the concentration of H atoms in solution during the anneals. This concentration may depend on the details of the procedure used to induce the dichroism, which involves a heat treatment in air at 420 $^{\circ}\text{C}$ for 30 min while the sample was under stress. It has been demonstrated that the rate of cooling from 420 $^{\circ}\text{C}$ can produce variations in the magnitude of the subsequently measured values of D_{oxy} and differences relating to different materials have been noted.⁶⁶ In summary, the observed scatter is greater than reported previously⁵¹ for samples heated at 900 $^{\circ}\text{C}$. These latter data are in good agreement with early results of Stavola *et al.*,⁷ described by

$$D_{\text{oxy}} = 3.2 \times 10^{-4} \exp(-1.96 \text{ eV/kT}) \text{ cm}^2 \text{ s}^{-1}$$

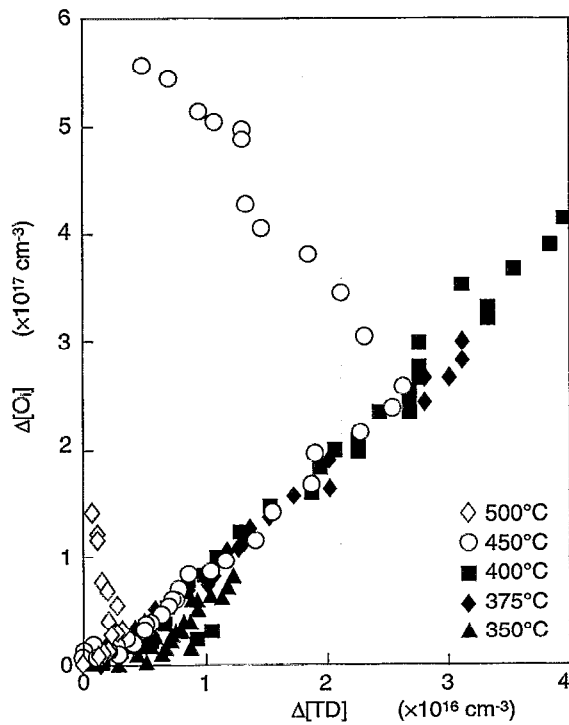


FIG. 9. Oxygen loss from solution as a function of increasing [TD] in samples prepared from crystal B annealed at (▲) 350, (◆) 375, (■) 400, (○) 450, and (◇) 500 °C. The data for the lowest anneal temperature appear to be displaced below those for anneals at the higher temperatures but the corresponding slopes are similar.

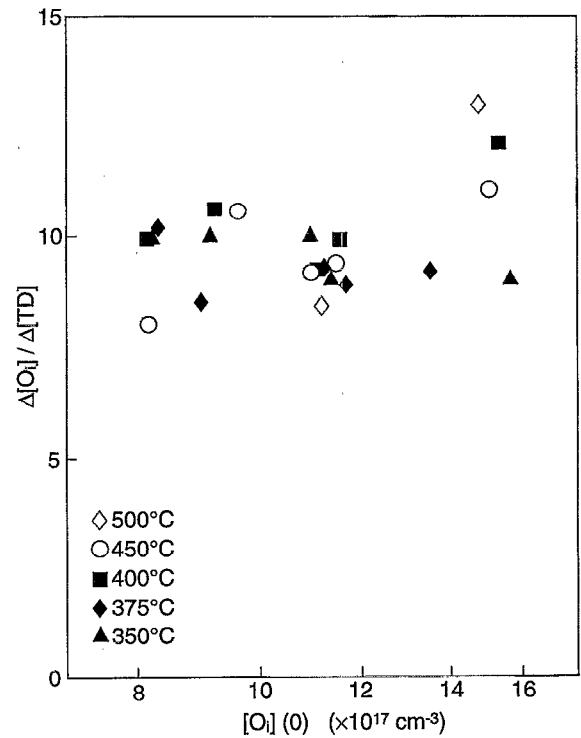


FIG. 10. The number of oxygen atoms lost from solution per thermal donor formed in samples annealed at (▲) 350, (◆) 375, (■) 400, (○) 450, and (◇) 500 °C as a function of the initial value of $[O_i]$.

(the dashed line in Fig. 11), relating to samples that had also been preheated at 900 °C, although a least-squares fit to all our data yielded

$$D_{\text{oxy}} = 2.0 \times 10^{-6} \exp(-1.68 \text{ eV/kT}) \text{ cm}^2 \text{ s}^{-1}$$

(the dotted line in Fig. 11). Irrespective of this spread, the activation energy of enhanced diffusion is significantly smaller than that for normal diffusion (2.53 eV). We now show that enhanced long-range diffusion of oxygen also occurs in hydrogenated silicon during subsequent low-temperature anneals.

Samples cut from silicon crystals A and F were etched and heated in $\text{H}_2(\text{g})$ in a silica tube (all components and samples had been RCA cleaned⁶⁷) for 30 min at 1300 °C. The anneal was terminated by a rapid quench, by dropping the samples into silicone oil at room temperature. The hydrogenated samples prepared from crystal F, and those from crystal A in some cases, were then annealed isothermally in air, together with as-grown control samples. Anneals were carried out at temperatures in the range $320 \leq T \leq 460$ °C and measurements of $[O_i]$ and [TD] were made at each stage of the anneal.

The rates of $[O_i]$ loss in the material which had been subjected to the hydrogenation treatment were greater than in the corresponding as-grown control samples (Fig. 12) at all anneal temperatures. The derived values of D_{oxy} for as-grown controls (Fig. 13) were consistent with those described in the last section (Fig. 7), while greatly enhanced

values were deduced for the hydrogenated samples (Fig. 13). The relatively rapid loss of $[O_i]$ from solution in the hydrogenated material was not due to diffusion of oxygen to structural defects, which might have been generated by the quench treatment, since the rate of TD formation was also enhanced. In fact the ratio $\Delta[O_i]/\Delta[\text{TD}]$ (~ 10) was the same as that measured for the as-grown controls (Fig. 14). The rate of $[O_i]$ loss tended to decrease monotonically with increasing anneal time (Fig. 15) and there were corresponding reductions in the rate of TD formation so that $\Delta[O_i]/\Delta[\text{TD}]$ was independent of anneal time until a maximum value of [TD] was established. These observations provide no evidence to support the suggestion that nuclei⁶⁸ required for TD formation were annealed during the high-temperature pretreatment but are fully consistent with the view that enhanced rates of TD formation can be attributed to catalyzed oxygen diffusion.^{57-59,69,70}

The enhancement mechanism which gave rise to increased rates of relaxation of stress-induced dichroism has now been shown to endure for times sufficient to cause substantial $[O_i]$ loss and the enhancement factors for the two processes at a given temperature are very similar (cf. Figs. 11 and 13). The enhancements did not depend on $[O_i]_{(0)}$ (see data for 320 and 375 °C in Fig. 13) indicating that the process was catalyzed by some impurity or defect other than oxygen. The monotonic decreases in the rate of $[O_i]$ loss (Fig. 15) can be attributed to the loss from solution of the species responsible for the enhancement. The present and

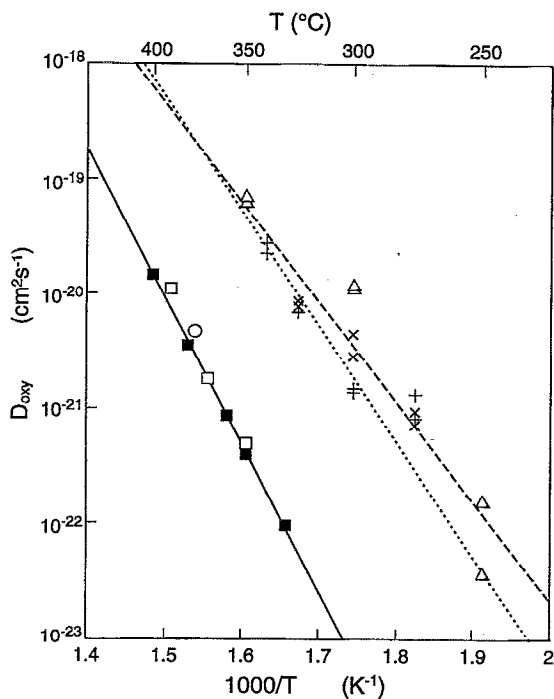


FIG. 11. Measurements of normal oxygen diffusion in as-grown material of (○) Corbett and co-workers (Ref. 3) (■) Stavola *et al.* (Ref. 7), and (□) Newman and co-workers (Ref. 8) (also shown in Fig. 1) together with enhanced values obtained in the case of material that had been preheated in $H_2(g)$ at (×) 800, (+) 900, and (△) 1300 °C then quenched to room temperature. The line fitted to all the data is shown (dotted line) given by $3.2 \times 10^{-4} \exp(-1.96 \text{ eV}/kT) \text{ cm}^2 \text{ s}^{-1}$ together with that fitted to previously reported enhancements (Ref. 7) (dashed line) given by $2.0 \times 10^{-6} \exp(-1.68 \text{ eV}/kT) \text{ cm}^2 \text{ s}^{-1}$ and the solid line represents normal oxygen diffusion (Fig. 1).

previous data support the identification of the catalyst as atomic hydrogen.

If a small concentration of hydrogen atoms were present in the as-grown material, the hydrogen enhancement mechanism might account for the correspondingly small initial enhancements implied by our analysis. The enhancement would be expected to decay as the concentration of hydrogen in solution became depleted during extended anneals, and normal oxygen diffusion should then be observed. This could account for the tendency of slopes of plots of $([O_i]^{-1})_{(t)}$ for anneals at 400 °C to decrease by a factor of ~ 3 after which they remained constant within the errors of the measurements (Fig. 15). Finally, we note that there is existing evidence for the loss of the effectiveness of hydrogen in enhancing oxygen diffusion after extended anneals derived from measurements of stress-induced dichroism.⁵⁸

IV. MODELING OF OXYGEN LOSS

The analysis based on second order kinetics [Eq. (3)] provides a self-consistent explanation for the experimental results for anneals at low temperatures ($T \leq 400$ °C). The rates of $[O_i]$ loss for anneals at higher temperatures were reduced (Fig. 7), resulting in a dependence on increasingly high powers of $[O_i]$ (Fig. 3). To investigate the role of dis-

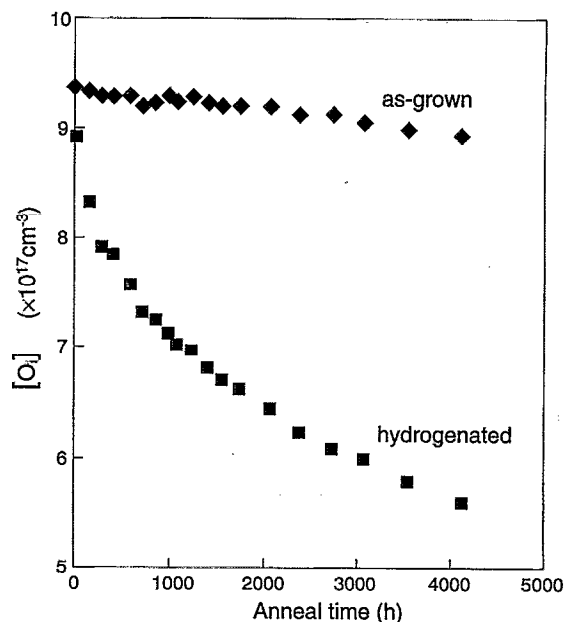


FIG. 12. (◆) Interstitial oxygen concentration as a function of anneal time at 350 °C for as-grown material prepared from crystal F and (■) a sample from the same crystal which had been heated to 1300 °C for 30 min in $H_2(g)$ and rapidly quenched to room temperature prior to the anneals.

sociative processes, a more detailed model of oxygen clustering which describes the evolution of oxygen clusters during anneals is required. As a first approximation, the process was assumed to occur by the serial reaction



where O_1 and O_m represent an O_i atom and a cluster of m oxygen atoms, respectively. The concentration of each cluster and the loss of $[O_i]$ from solution could be computed iteratively if reasonable assumptions were made about the starting conditions and the diffusion processes which control the reaction rates.

As in the previous kinetic model of Tan and co-workers,⁴² all clusters (including O_2 dimers) were initially taken to be immobile, so that the rate of each forward step in the reaction would be controlled by the diffusivity of O_1 atoms and the normal value of D_{oxy} at 450 °C was chosen. The forward rate constant was derived as $k_f = 4\pi r_c D_{oxy}$ and r_c was taken to be 5 Å, independent of cluster size. The rate of oxygen loss was then given by

$$-\frac{d[O_1]}{dt} = -2k_f[O_1]^2 - k_f[O_1] \sum_{m=2}^{M-1} [O_m], \quad (5)$$

where the first term represents the dimerization process [see Eq. (3)] and the second term represents the diffusion of O_1 atoms to larger clusters containing 2 or more (up to M) oxygen atoms. Oxygen trapping by the largest cluster O_M , was neglected so that larger clusters could not form. The net rate of dimer formation was described by

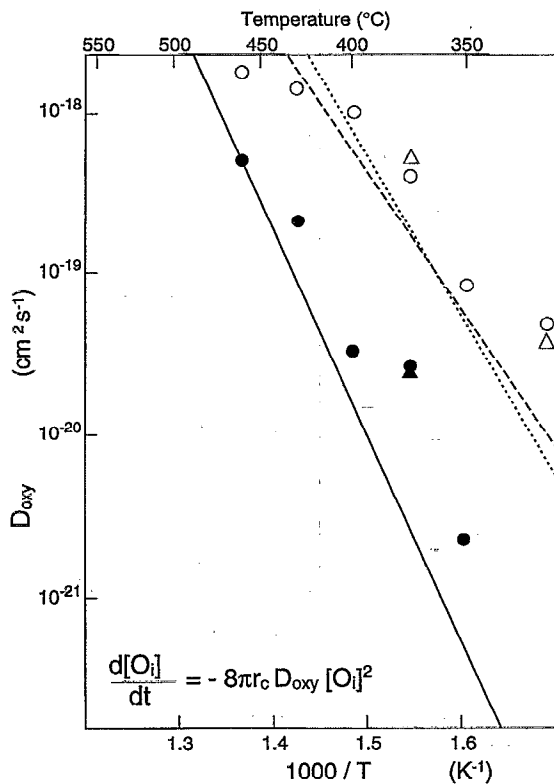


FIG. 13. An Arrhenius plot of the values of D_{oxv} derived from the gradients of graphs of $([O_i]^{-1})_t$ for as-grown samples prepared from crystals (▲) A and (●) F and the corresponding values for samples cut from crystals (△) A and (○) F which had been heated to 1300 °C for 30 min in $H_2(g)$ prior to the anneals. The solid line represents an extrapolation of normal values of D_{oxv} given by $0.13 \exp(-2.53 \text{ eV}/kT) \text{ cm}^2 \text{ s}^{-1}$ while the dashed and dotted lines represent two extrapolations of the dichroism measurements (Fig. 11) of enhanced D_{oxv} .

$$\frac{d[O_2]}{dt} = k_f [O_1]^2 - k_f [O_1][O_2], \quad (6)$$

while the formation of larger clusters ($m > 2$) was given by

$$\frac{d[O_m]}{dt} = k_f [O_1][O_{m-1}] - k_f [O_1][O_m]. \quad (7)$$

A dispersed solution of 10^{18} cm^{-3} O_1 atoms was presumed to exist prior to the anneals and the concentrations of clusters containing up to $M = 10$ O atoms were calculated by integrating the reaction rates during a simulated anneal which was continued until $[O_1]$ decreased by 20%. During the anneals, around 90% of the O_1 atoms lost from solution were incorporated as O_2 dimers and the concentrations of larger clusters decreased by about an order of magnitude on increasing cluster size from m to $m+1$ [Fig. 16(a)], consistent with the results of previous modeling.⁴² The effect of terminating the clustering for large clusters O_M , would not significantly affect the evolution of the smaller clusters since their concentrations were always much greater than $[O_M]$. A plot of $([O_1]^{-1})_t$ was linear and the gradient was very close to $8\pi r_c D_{\text{oxv}}$ since $[O_1]$ loss was controlled primarily by O_2 dimer formation rather than by diffusion to clusters. This model would, therefore, be consistent with the use of Eq. (3)

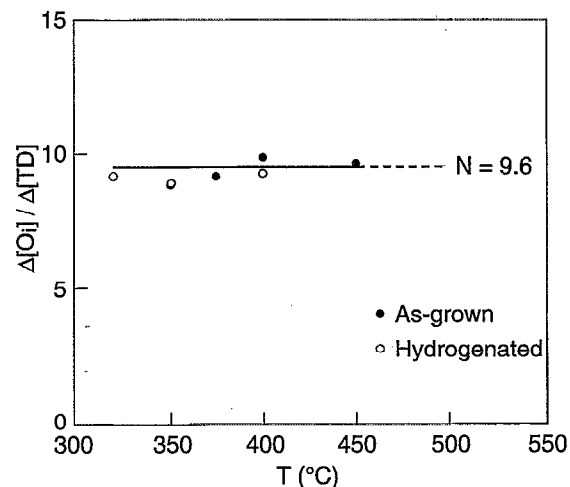


FIG. 14. The average ratio of the concentration of oxygen lost from solution relative to the concentration of TDs formed in (○) as-grown and (●) hydrogenated samples as functions of anneal temperature.

to derive values of D_{oxv} from measurements of $[O_i]$ loss during low-temperature ($T \leq 400$ °C) anneals (Sec. II).

Dissociative processes are required to explain observations relating to anneals at higher temperatures ($T \geq 450$ °C), as already mentioned. Further calculations were made with

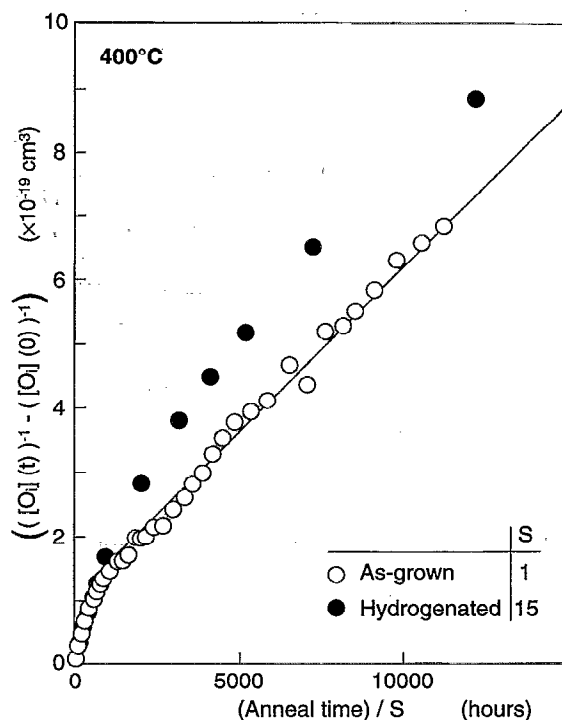


FIG. 15. The oxygen loss data plotted in the form $([O_i]^{-1})_t$ and normalized by subtracting the inverse of the initial oxygen concentration for the (○) as-grown and (●) hydrogenated samples annealed at 400 °C as functions of anneal time divided by the scaling factor S chosen so that the initial gradients were the same. The straight line illustrates the constant slope of the data for as-grown material during extended anneals.

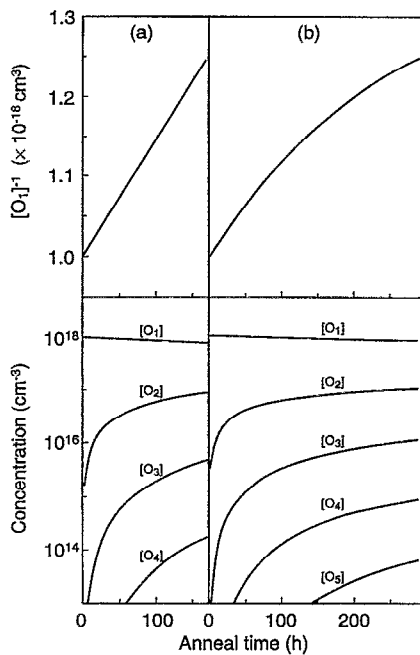


FIG. 16. Variations in $([O_1]^{-1})^{(t)}$ (upper plots) together with the evolution of $[O_1]$ and larger clusters (lower plots) as functions of simulated anneal time starting from a completely dispersed solution based on a model of immobile clusters which were considered to be (a) stable and (b) dissociating at a rate of 10^{-6} s^{-1} .

the assumption that all clusters dissociated with the same rate coefficient k_r , to form O_{m-1} by the release of an O_1 atom into solution. The process was incorporated in the model by adding the extra terms $k_r(2[O_2] + \sum [O_m])$, $k_r([O_3] - [O_2])$, and $k_r([O_{m+1}] - [O_m])$ to Eqs. (5), (6), and (7), respectively. The results of the simulation using a value of $k_r = 10^{-6} \text{ s}^{-1}$ [Fig. 16(b)] demonstrate that while the initial gradient of a plot of $([O_1]^{-1})^{(t)}$ was not affected, the inclusion of the dissociation process caused the slope of the plot to decrease continuously with increasing time. This behavior is easily understood since, in the early stages of the anneals, the concentrations of clusters leading to reverse reactions were negligible compared with $[O_1]$. The effect of dissociation became more pronounced during the anneals as the concentrations of clusters increased, leading to a slowing down of the whole aggregation process. The inclusion in the modeling of dissociation in this way does not, therefore, account for the experimentally observed reductions of the initial slope of $([O_1]^{-1})^{(t)}$ and there is no experimental evidence for increased curvature of the data at the higher temperatures (Fig. 8).

If O_2 dimers were much less stable than larger clusters ($m > 2$) then a quasiequilibrium dimer concentration $[O_2]_{\text{eq}}$ would be established ($d[O_2]_{\text{eq}}/dt \rightarrow 0$), while the concentrations of larger clusters would continue to increase with anneal time. Calculations using a dimer dissociation rate $k_{r2} = 4 \times 10^{-6} \text{ s}^{-1}$ (Fig. 17) demonstrate that a plot of $([O_1]^{-1})^{(t)}$, which initially had a slope that was indistinguishable from that obtained in the absence of dissociation, subsequently tended to a linear variation with a gradient that

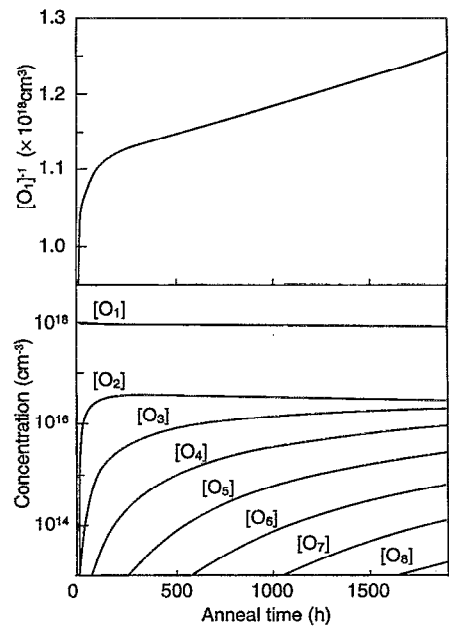


FIG. 17. Variations in $([O_1]^{-1})^{(t)}$ (upper plot) together with the evolution of $[O_1]$ and larger clusters (lower plot) as functions of simulated anneal time based on a model of immobile clusters and assuming a dimer dissociation rate of $2 \times 10^{-6} \text{ s}^{-1}$.

was smaller than $8\pi r_c D_{\text{oxy}}$ by a factor of ~ 20 . This transition occurred when $[O_2]_{\text{eq}}$ had been established and thereafter the slope of the plot did not change because $[O_2]_{\text{eq}}/[O_1]$ remained constant. In this latter stage the modeled $[O_1]$ -loss process followed third-order kinetics (i.e., $d[O_1]/dt$ varied as $[O_1]^3$) so that the apparent value of D_{oxy} derived using second-order kinetics varied linearly with $[O_1]_{(0)}$, consistent with the functional dependence observed for anneals at $\sim 450^\circ \text{C}$ (Figs. 3 and 5); however, estimates of D_{oxy} derived in this way would be 20 times smaller than the real value. Since those derived from measurements were close to normal for $T = 450^\circ \text{C}$ (Fig. 7), D_{oxy} would have had to have been enhanced by this large factor, inconsistent with the results of the corresponding analysis for anneals at 400°C . Another major problem is that there is no experimental evidence for the initial rapid transient extending for $\sim 100 \text{ h}$ and involving the loss of $\sim 10\%$ of $[O_1]$ from solution, predicted by the modeling (Fig. 17). This absence could in principle be explained if $[O_2]_{\text{eq}}$ had already been established prior to the anneals; however, anneals at 1300°C in argon gas followed by a rapid quench to room temperature did not affect the value of $[O_i]$ in samples prepared from each of the crystals used in this work, implying that the concentration of oxygen in clustered form was much smaller than the value of $[O_i]$ in the as-grown state; furthermore, the initial transient was also absent for anneals of hydrogenated samples, which had been subjected to a similar thermal pretreatment. While the $[O_i]$ loss associated with the initial transient would be smaller if the real value of k_{r2} was greater than that used in the modeling, the slopes of plots of $([O_1]^{-1})^{(t)}$ would then imply even more dramatic increases in the enhancement of D_{oxy} on increasing the temperature from 400 to 450°C .

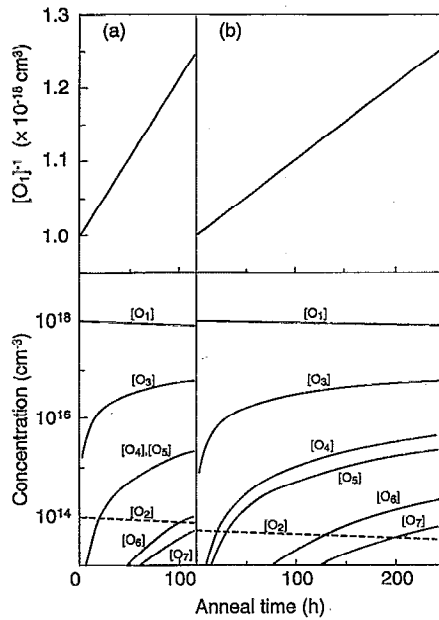


FIG. 18. Variations in $([O_1]^{-1})_{(t)}$ (upper plots) together with the evolution of $[O_1]$ and larger clusters (lower plots) as functions of simulated anneal time based on a model of rapid dimer diffusion ($D_{O_2}/D_{O_1} = 10^4$) (a) where all clusters were assumed to be stable and (b) for a dimer dissociation rate of $2 \times 10^{-2} \text{ s}^{-1}$. The effect of dimer dissociation is to reduce the rate of $[O_1]$ loss without affecting the form of the data nor the sizes of clusters that form during the anneals.

The important point to emerge from this aspect of the modeling was that the existence of a quasiequilibrium dimer concentration offered an explanation for the observed dependency of $d[O_i]/dt$ on a third power of $[O_i]_{(0)}$ while conserving the linear form of plots of $([O_1]^{-1})_{(t)}$. We now show that a quasiequilibrium dimer concentration can be established even if dimer dissociation is not significant, if O_2 dimers are assumed to diffuse much more rapidly than single O_1 atoms. Rapid dimer diffusion was incorporated in the model by addition of the further terms

$$-k_{f2}[O_2][O_1],$$

$$-k_{f2}[O_2]([O_1] + 2[O_2] + \Sigma[O_m]),$$

and

$$k_{f2}[O_2]([O_{m-2}] - [O_m])$$

to Eqs. (5), (6), and (7), respectively. The forward rate constant $k_{f2} = 4\pi r_c D_{O_2}$ represents the contribution to cluster formation caused by dimer diffusivity D_{O_2} and a ratio of $D_{O_2}/D_{O_1} \sim 10^4$ was chosen to illustrate the effects of this process. If all clusters ($m \geq 3$) were stable ($k_r = 0$), plots of $([O_1]^{-1})_{(t)}$ were linear [Fig. 18(a)] and the gradient was greater than $8\pi r_c D_{O_1}$ by a factor of 3/2. This effect arises because the formation of an O_2 dimer would be followed by its rapid diffusion, predominantly to another O_1 atom resulting in O_3 formation. Thus, the process would follow second-order kinetics, consistent with experimental observations for anneals at low temperatures, and the small increase in rate might imply smaller enhancements of D_{O_1} than the factor of

~ 3 derived in Sec. II. In contrast to the immobile dimer model, a quasiequilibrium value of $[O_2]$ was quickly established and remained constant relative to $[O_1]$ throughout the anneals [Fig. 18(a)]. Therefore, $[O_1]$ loss led only to increases in the concentrations of immobile clusters with $m \geq 3$.

With the assumption of a high rate of dimer dissociation ($k_{r2} = 2 \times 10^{-2} \text{ s}^{-1}$), in addition to rapid dimer diffusion, neither the linearity of plots of $([O_1]^{-1})_{(t)}$ nor the sizes of clusters that formed during the anneals were affected, but the overall rate of the process was reduced [Fig. 18(b)]. This behavior is consistent with the experimentally observed reduced rates of $[O_i]$ loss without changes in the form of the variation with anneal time. Such reductions would be significant at temperatures at which the dissociation rate exceeded the rate of trapping of the diffusing dimer by an O_1 atom. Since trimers were assumed to be stable, $[O_3]$ increased with anneal time and, by ignoring the role of larger ($m > 3$) clusters, the quasiequilibrium dimer concentration, defined by $d[O_2]/dt = 0$, can be shown to satisfy the relation

$$[O_2]_{eq} = k_{f1}[O_1]^2 / (k_{r2} + [(k_{f2} + k_{f1})[O_1]]),$$

so that

$$\frac{d[O_1]}{dt} = \frac{-3k_{f1}k_{f2}[O_1]^3}{[(k_{f2} + k_{f1})[O_1] + k_{r2}]}.$$

At low temperatures at which dimer dissociation would be insignificant [$k_{r2} \ll (k_{f2} + k_{f1})[O_1]$] the value of $[O_2]_{eq}$, controlled by the balance between formation and diffusion to O_1 atoms, would vary linearly with $[O_1]$ in different samples and $d[O_1]/dt$ would be proportional to $[O_1]^2$. At higher temperatures at which dimers would be more likely to dissociate than to diffuse to an O_1 atom [$k_{r2} \gg (k_{f2} + k_{f1})[O_1]$], the value of $[O_2]_{eq}$ would be reduced, tending to a value of $(k_{f1}/k_{r2})[O_1]^2$ and $d[O_1]/dt$ would be proportional to $[O_1]^3$. Thus, the apparent order of the clustering process depends on the relative rates of dimer dissociation and their diffusion to traps. The observed increase in this apparent order from two to three as the anneal temperature was increased from 400 to $\sim 450^\circ \text{C}$ (Fig. 3) can be explained in this way, without implying that clusters of different sizes were predominantly formed during the anneals at the different temperatures. This is a unique feature of the rapidly diffusing dimer model and helps to account for TD formation, as discussed later.

Although further increases in the value of k_{r2} would lead to larger reductions in the rate of $[O_1]$ loss, the net rate of the process would remain proportional to $[O_1]^3$ according to the model outlined so far and so it is not possible to account for the observation that $d[O_i]/dt$ varies with even higher powers of $[O_i]$ for anneals at $T \geq 450^\circ \text{C}$ (Fig. 3). This behavior suggests that $[O_1]$ loss is due predominantly to increases in the concentrations of relatively large oxygen clusters. It is next necessary to investigate whether the foregoing assumption that O_3 defects were stable is a necessary requirement for the essentially new features of the modeling. If trimers dissociated at a high rate k_{r3} , their concentration would also reach quasiequilibrium $[O_3]_{eq}$, during the early stages of the anneals. Provided the total concentration of oxygen in dimer and trimer form was not measurable ($< 10^{16} \text{ cm}^{-3}$) then the incubation period (see Fig. 17) required to establish $[O_2]_{eq}$

and $[O_3]_{eq}$ would not be observed experimentally. The quasiequilibrium dimer concentration would be controlled at low temperatures by the balance between the rates of their formation and their rapid diffusion to another dimer or a trimer, depending on the relative values of $[O_2]_{eq}$ and $([O_3]_{eq}/2)$ assuming that larger clusters (O_4 and O_5) are stable. Once quasiequilibrium had been established only two O_1 atoms would be lost from solution for each dimer formed so the slope of plots of $([O_1]^{-1})_{(t)}$ would be close to $2k_{f1}$, as assumed in our simple analysis (Secs. II and III). In other words, the observation that $d[O_i]/dt$ follows second-order kinetics at low temperatures (Fig. 3) requires only that the rate of dimer dissociation is less than the rate at which rapidly diffusing dimers are trapped to form stable clusters. There is no requirement that intermediate-sized clusters such as O_3 are stable and the results for anneals at low temperatures would provide no information about the size of cluster formed as a result of dimer diffusion.

At higher temperatures dimers become increasingly likely to dissociate before being trapped to form a stable cluster. Values of $d[O_1]/dt$ would therefore be lower than expected if dissociation had not occurred. As already described in the case where trimers were considered to be stable, dimer dissociation would lead to an apparent transition to higher-order kinetics. We now consider the possibility that dimer trapping occurs mainly as a result of dimer-trimer interactions resulting in the formation of stable O_5 clusters. Ignoring the trapping of dimers by larger clusters, the process can be described by a series of kinetic equations. By setting $d[O_3]/dt=0$ the expression

$$[O_3]_{eq} = (k_{f2}[O_2]_{eq}[O_1]) / (k_{r3} + k_{f2}[O_2]_{eq})$$

is obtained. Repeating this procedure for $d[O_2]/dt$ then leads to a quadratic expression in $[O_2]_{eq}$ that has only one positive root. For a negligible rate of dimer dissociation, $[O_1]=1 \times 10^{18} \text{ cm}^{-3}$ and $k_{r3}=5 \times 10^{-4} \text{ s}^{-1}$, and using the same values of k_{f1} and k_{f2} as those chosen for our modeling, $[O_2]_{eq}$ and $[O_3]_{eq}$ can be calculated as 3.6×10^{15} and $1.4 \times 10^{16} \text{ cm}^{-3}$, respectively. This value of $[O_2]_{eq}$ is much higher than that obtained under the assumption that O_3 were stable (Fig. 18), because the rate at which dimers are trapped is significantly reduced by the inclusion of a high trimer dissociation rate. In fact these values of $[O_2]_{eq}$ and $[O_3]_{eq}$, would be sufficiently large to account for all of the first $\sim 10\%$ of $[O_1]$ loss assuming a dispersed solution of $[O_1]$ atoms existed prior to the anneals. The effect of trimer dissociation would then not be significant until a time corresponding to that at which $[O_3]$ tended to quasiequilibrium. This incubation time would be insignificant relative to the time required to measure the first 10% of $[O_1]$ loss, if the amount of oxygen incorporated as $[O_2]_{eq}$ and $[O_3]_{eq}$ was much smaller than $([O_1]/10)$. This requirement implies that the real value of the ratio D_{O_2}/D_{oxy} would have to be much greater than that of 10^4 used in these calculations. Irrespective of this issue, further calculations for different values of $[O_1]$ confirmed that $d[O_1]/dt$ and $d[O_5]/dt$ varied with $[O_1]^2$. This result is reasonable since the rate of $[O_1]$ loss would be

limited by the rate of O_2 dimer formation, regardless of the size of clusters formed due to the clustering of rapidly diffusing dimers.

To simulate the effect of increasing the temperature of the anneals, calculations were repeated for increasing values of k_{r2} . A value of $k_{r2}=1 \times 10^{-5} \text{ s}^{-1}$ caused a 15% reduction in $d[O_1]/dt$ which then varied with $[O_1]^{2.3}$, a change which would be too small to resolve experimentally. Higher values of k_{r2} led to increases in the magnitude of these changes and a value of $k_{r2}=4 \times 10^{-4} \text{ cm}^{-2}$ led to reductions of almost an order of magnitude in $[O_2]_{eq}$ and $[O_3]_{eq}$ (4.9×10^{14} and $2.0 \times 10^{15} \text{ cm}^{-3}$, respectively) while both $d[O_1]/dt$ and $d[O_5]/dt$ were reduced by a factor of ~ 50 and tended to vary with $[O_1]^{4.8}$. The magnitude of this reduction is similar to the difference between the average measured rate of $[O_i]$ loss and that expected from second-order kinetics for anneals at 500°C (Fig. 7). Even larger increases in k_{r2} led to greater reductions in the $[O_1]$ -loss rate but the dependence on $[O_1]^n$ did not increase above $n=5$. The calculations show that the maximum apparent order of the $[O_i]$ -loss process, observed as the temperature is increased, can be related to the size of the smallest cluster which is stable during the anneals.

The observed tendency of $d[O_i]/dt$ to vary with $[O_i]^8$ at 500°C can therefore be explained if dimer clustering leads predominantly to the increasing concentration of aggregates containing as many as eight oxygen atoms. Changes in the apparent kinetics for temperatures below 500°C can then be explained by reduced rates of dissociation relative to formation of dimers (k_{r2}/k_{f1}) without affecting the sizes of oxygen clusters that form during the anneals. Note that a much larger value of D_{O_2}/D_{oxy} than 10^4 would be required if $[O_i]$ loss led mainly to increases in the concentration of such large clusters. Otherwise a significant incubation stage of $[O_i]$ loss would be expected, prior to the establishment of quasiequilibrium concentrations of the intermediate-sized oxygen clusters.

The internal strain in the large clusters formed during the anneals may cause the ejection of one or more self-interstitials into the surrounding matrix. These rapidly diffusing defects could interact with O_2 dimers forming a stable and immobile $O_2\text{-Si}_i$ complex, as has been suggested previously.⁴⁰ In view of the results of our modeling, they might also interact with other small clusters present in quasiequilibrium concentrations. We have included reactions of this type in various further models but have found that the dependency of $d[O_1]/dt$ on $[O_1]_{(0)}$ was not affected. It would appear then that the $[O_i]$ -loss measurements would not be expected to provide evidence for such processes.

The modeling has led to a new and rather unconventional description of the oxygen-loss process at these low temperatures. The central idea is that oxygen dimers, which diffuse relatively rapidly, act as precursors to the growth of relatively large oxygen clusters. Although the formation of such large clusters might be expected for anneals at the highest temperature, the apparent changes in the order of the process for anneals at lower temperatures can be explained without implying changes in size of the clusters formed during the anneals. The behavior can be attributed to a decreasing rate of dimer dissociation relative to that of formation as

the temperature is reduced. Note that the intermediate clusters which would be present in quasiequilibrium concentrations are not necessarily required to be less stable than O_2 since the dimer lifetime may be much smaller due to its high diffusion rate and subsequent trapping. However, it is also possible that the barrier to dissociation of clusters larger than O_2 by release of O_2 may be lower than for the release of O_i , given that the barrier for O_2 diffusion would appear to be much lower; thus, the relative stability of intermediate-sized oxygen clusters might be similar over a wide temperature range (350–500 °C).

V. DISCUSSION

The size of oxygen clusters that form during anneals at temperatures below 650 °C has not been determined directly.¹⁶ Analysis of $[O_i]$ loss during such anneals relies on the use of an assumed model which must be shown to provide a self-consistent explanation of the process. The rate of $[O_i]$ loss at low temperatures ($T \leq 400$ °C) has been shown in this work to be proportional to $[O_i]^2$ (Fig. 3). The use of second-order kinetics with a reasonable choice of $r_c = 5$ Å led to values of D_{oxy} which were only a factor of ~ 3 greater than normal (Fig. 7). Support for the small apparent enhancement was provided by the form of plots of $([O_i]^{-1})_{(t)}$ (Figs. 6 and 8) which suggested that the initial value of D_{oxy} decreased by a factor of ~ 3 before remaining relatively constant with increasing anneal time (Fig. 15). Deliberate hydrogenation of material led to much greater enhancement factors of around 100 at 350 °C (Fig. 13), although the degree of enhancement tended to decrease slowly with increasing anneal time (Fig. 15). The previously reported catalysis of oxygen diffusion jump rates^{7,51,52} (Fig. 11) have thereby been shown to persist for sufficiently long times to cause a measurable loss of $[O_i]$ from solution. These results demonstrate beyond reasonable doubt that the rate-limiting step in the $[O_i]$ -loss process at these low temperatures was due to O_i - O_i interaction.

The catalyst responsible for the small enhancements during the early stages of the anneals does not appear to be related to a defect generated by, or consumed during, the $[O_i]$ -loss process since the degree of enhancement was independent of $[O_i]_{(0)}$ (Fig. 13). Other work⁵⁹ relating to heat treatments of samples in plasmas provides evidence that the process probably involves transient interactions between O_i atoms and rapidly diffusing H atoms. Features commonly detected in photoluminescence⁷¹ and IR-absorption⁷² spectra of as-grown material have recently been shown to incorporate hydrogen, demonstrating that it is a residual contaminant. The present results might be explained if some of this hydrogen can be released into solution during heat treatments but the degree of dissolution decreases with increasing anneal time.

The rates of $[O_i]$ loss for anneals at higher temperatures ($T \geq 450$ °C) were lower than expected (Fig. 7) and the reductions were greatest for samples with lowest values of $[O_i]_{(0)}$ (Fig. 5). Values of D_{oxy} derived using second-order kinetics therefore appeared to increase with $[O_i]_{(0)}$, consistent with previous observations for anneals at ~ 450 °C.^{42,43} The fact that the form of plots of $([O_i]^{-1})_{(t)}$ was not different

from that at lower temperatures (Fig. 8) could be explained if the dissociating cluster was present in a quasiequilibrium concentration throughout the anneals. If all clusters were assumed to be immobile, a quasiequilibrium dimer concentration could be established as a result of dimer dissociation but the measured rates of $[O_i]$ loss would then require enhancements of D_{oxy} far in excess of those derived for anneals at only slightly lower temperatures ($T \leq 400$ °C). This problem could be avoided if O_2 dimers were assumed to diffuse much more rapidly than isolated oxygen atoms so that a quasiequilibrium value of $[O_2]$ was established even at the lower temperatures at which dissociation was insignificant. The dependence of $d[O_i]/dt \propto [O_i]^8$ for anneals at 500 °C implied that the concentrations of clusters containing fewer than ~ 8 O atoms were in quasiequilibrium during the anneals, due to the balance between their formation and dissociation. The $[O_i]$ -loss process over the whole range of temperatures could then be explained by increases in the ratio of the rate of dimer dissociation relative to that of their formation as the temperature was increased, with no requirement for the formation of larger oxygen clusters at the higher temperatures.

Although the possibility that O_2 dimers might diffuse more rapidly than O_i atoms has been considered for many years, there is no unambiguous evidence that such rapid diffusion occurs. Since our analysis of the $[O_i]$ -loss kinetics appears to require this process, we now consider whether other experimental results might provide further support. It is interesting to recall the results of heating Si containing both oxygen ($[O_i] \sim 10^{18}$ cm⁻³) and substitutional carbon ($[C_s] \sim 10^{18}$ cm⁻³). The rate of $[O_i]$ loss during anneals at 450 °C was not measurably different from that for low-carbon material,^{10,43} but this result was not surprising since the diffusivity of C_s is negligible at this low temperature and the concentration of C_s - O_i complexes increased only slightly during the anneals. In other words, the rate-limiting step for $[O_i]$ loss did not appear to have been affected by the presence of high levels of $[C_s]$, but remained due to O_i - O_i interaction. However, the rate of TD formation was much (up to a factor of 100) lower than for low carbon material,⁷³ leading to corresponding increases⁷⁴ in $\Delta[O_i]/\Delta[TD]$, and $[C_s]$ was lost from solution at half the rate of $[O_i]$ loss.¹⁰ This latter observation was previously explained by the following sequence of reactions: (a) ejection of a rapidly diffusing self-interstitial Si_i upon O_2 formation; (b) exchange of sites between Si_i and C_s ; and (c) rapid diffusion of the interstitial carbon atom to O_2 pairs to form O_2 - C_i complexes. Evidence for the formation of such complexes has been provided by IR-absorption⁷³ and photoluminescence⁷⁵ spectroscopies. The main problem with this explanation is that calculations⁷⁶ indicate that there is insufficient strain within a cluster as small as O_2 to cause the ejection of a self-interstitial. We have now demonstrated that if rapid dimer diffusion occurs, the observations for carbon-doped material may alternatively be explained if the formation of relatively large oxygen clusters led to the ejection of several Si_i defects per cluster. In fact, rapid dimer diffusion might explain the observations without requiring the ejection of self-interstitials since O_2 - C_i complexes may form directly by the trapping of O_2 by C_s .

followed by the displacement of the carbon atom to an interstitial site.

Another observation relates to material that does not contain high levels of carbon. As absorption is lost from the 1107 cm^{-1} ($9\text{ }\mu\text{m}$) band due to decreases in $[\text{O}_i]$ during anneals, no absorption of comparable strength appears at similar frequencies in the IR spectrum. If dimer diffusion was insignificant then the occurrence of second-order kinetics, demonstrated in the present work, would lead to the expectation of a high concentration of stable $\text{O}_i\text{-O}_i$ pairs in material annealed at low temperatures. Since no strong absorption was detected, the dipole moment per unit displacement η of the O atoms in this defect would then have to be lower than the value of $\eta \sim 3.5e$, where e is the charge of an electron, for O_i , derived from the calibration of the $9\text{ }\mu\text{m}$ band. While the latter value is unusually high and values of $\eta \sim 1e$ have been derived from the absorption due to other impurities, there is no evidence for significant changes of η associated with O in different bond-centered positions. Thus, for O-vacancy centers, involving an extended Si—O—Si bridging bond, η is independent of the charge state of the defect⁷⁷ and is almost the same⁷⁸ as for O_i . The discrepancy might be explained if most of these clustered O atoms were present in a different bonding configuration with a low value of η . For example, a value of $\eta = 1$ would lead to the expectation of absorption which was less than that lost from the $9\text{ }\mu\text{m}$ band by a factor of ~ 12 .

In fact, we observed weak and broad IR absorption at $\sim 1013\text{ cm}^{-1}$ in the IR spectra of annealed samples that contained high concentrations of TD defects. In agreement with recent work,⁷⁹ the absorption in this band could be correlated with the values of $[\text{TD}]$. The strength, position, and form of the absorption was not significantly affected by cooling samples from 350 to 6 K and so the origin of the line can be assumed to be due to a vibrational rather than an electronic transition(s). The absorption may originate from Si-O vibrations in the cores of TD defects⁷⁹ since electron nuclear double-resonance measurements have provided evidence that they contain at least two O atoms;^{80,81} however, a shift of the vibrational frequency might have been expected as the sample temperature was reduced from room temperature due to changes in the charge state of the TDs. Our measurements indicate that an integrated absorption coefficient, $\int \alpha d\nu$, of 1 cm^{-2} in the 1013 cm^{-1} band is equivalent to $[\text{TD}] = 1.6 \times 10^{16}\text{ cm}^{-3}$. By comparison with the 1107 cm^{-1} band for which $\int \alpha d\nu = 1\text{ cm}^{-2}$ corresponds to $[\text{O}_i] = 1.0 \times 10^{16}\text{ cm}^{-3}$, this calibration would imply an average of ~ 0.6 or 7 O atoms per donor, depending on whether η was $3.5e$ or $1e$, respectively. Since $\sim 10\text{ O}_i$ atoms were lost from solution per TD formed during the early stages of the anneals, the 1013 cm^{-1} band could account for the loss of $[\text{O}_i]$ if η was small. It is worth noting that we also detected room-temperature IR absorption at a relatively low frequency of $\sim 740\text{ cm}^{-1}$ in samples with high $[\text{TD}]$; this absorption might be related to vibrational bands detected previously⁸² at 728 and 770 cm^{-1} in spectra obtained at low temperatures and believed to be associated with TD defects. These observations might be explained if clustered oxygen was threefold coordinated as suggested by calculations.^{47,49,50} Such bonding arrangements

have been invoked to explain not only thermal donor behavior but also rapid dimer diffusion.

Although D_{oxy} might also be enhanced during the early stages of anneals at $T \geq 450^\circ\text{C}$, as it appears to be at lower temperatures, the form of plots of $([\text{O}_i])_{(t)}$ versus anneal time are not more linear (Fig. 8) as might have been expected if the enhancement had decreased as the temperature was increased (Fig. 11); however, given that dimer dissociation appears to become increasingly important at the higher temperatures, small increases in $[\text{O}_2]_{\text{eq}}/[\text{O}_1]$ with increasing anneal time may also contribute to the curvature of the data for $T \geq 450^\circ\text{C}$. The fact that the slope of an Arrhenius plot ($\sim 1.8\text{ eV}$) of $d[\text{O}_i]/dt$ has been found^{44,45} to be lower than the activation energy of normal oxygen diffusion (2.53 eV) can be attributed to the combined effects of dimer dissociation for $T \geq 450^\circ\text{C}$ and the extrinsic enhancement of D_{oxy} at lower temperatures. Since TD formation appears to be controlled by the rate of $[\text{O}_i]$ loss (Figs. 3, 9, 10, and 14), the same explanation should account for the similarly low slope of an Arrhenius plot of $d[\text{TD}]/dt$.^{44,45,83–85}

It is well known that TDs are not unique defects and consist of a series of as many as 16 different centers⁸⁶ formed consecutively⁸⁷ in a sequence that is unchanged⁸³ for anneals at temperatures in the range of $400 \leq T \leq 500^\circ\text{C}$. The formation of such a plethora of centers could not occur if most of the O_i atoms lost from solution remained as uncomplexed O_2 . Our modeling of oxygen loss, based on rapid dimer diffusion, demonstrates how a series of different sizes of oxygen clusters might form during anneals over the whole temperature range $350 \leq T \leq 500^\circ\text{C}$. It is, therefore, possible that the different individual donor centers might be various sizes of oxygen clusters. The fast-diffusing species,⁶⁸ which converts a TD to the next in the series, might then be identified as the O_2 dimer.

Recent evidence from measurements of the NL8 electron paramagnetic-resonance spectrum indicates that the number of O atoms in TD centers increases after extended anneals.⁸⁸ Although this work is not yet quantitative and the actual number of O atoms was not specified, it was argued that chains of O_i atoms were formed along $[110]$ directions: in that case it is difficult to understand why the vibrational dipole moment should be low. Other work^{85,86} has shown that TDs present in samples can be destroyed upon subsequent annealing at $T \geq 600^\circ\text{C}$ and $\sim 8\text{ O}_i$ atoms are released into solution for each TD lost. If the more recent calibration⁵⁴ of the $9\text{ }\mu\text{m}$ IR band had been used, this figure would have been ~ 10 consistent with the present measurements relating to TD formation. Furthermore, the dependence of the maximum concentration of individual TDs on $[\text{O}_i]$ in different samples has been found^{87,89} to increase with their position in the series, at least in the cases of the earliest centers. All these observations can be explained if the different TD defects correspond to various sizes of oxygen clusters formed during the anneals. One problem with this interpretation arises since the number of O_i atoms lost per TD formed does not appear to change with $[\text{TD}]$ until a maximum value was established (Fig. 9) despite the fact that increasingly higher-order TDs have been shown to form during anneals,^{83,87,89} however, it should be noted that lines in the TD electronic spectrum

become increasingly difficult to resolve with increasing [TD] above $\sim 10^{16} \text{ cm}^{-3}$ whereas the ratio $\Delta[\text{O}_i]/\Delta[\text{TD}]$ is not easily determined during the early stages of the anneals (Fig. 9). Given these limitations, it is possible that the number of oxygen atoms lost from solution per donor formed does increase with anneal time but only during the early stages of the anneals.

Calculations suggest that the further incorporation of a self-interstitial may be necessary to account for donor behavior,^{49,76} raising the possibility that the rate of TD formation may be controlled by the generation of self-interstitials which, in turn, might result from the formation of large oxygen clusters and their subsequent relaxation to silicallike particles. In this respect it is worth noting that we have only been able to detect the presence of SiO_2 (giving rise to broad absorption at energies similar to that due to O_i) after $[\text{O}_i]$ loss has been continued beyond that required to establish a maximum value of [TD]. There is, therefore, no direct evidence for significant self-interstitial generation during TD formation although it must occur during more prolonged anneals to account for the RLDs observed by TEM.

VI. CONCLUSIONS

The analysis of measurements of $[\text{O}_i]$ loss and TD formation over a wide temperature range leads to a series of important conclusions. $\text{O}_i\text{-O}_i$ dimerization has been shown to be the rate-limiting step in the loss of isolated oxygen from solution during anneals at low temperatures ($T \leq 500^\circ\text{C}$). Oxygen diffusion appears to have been enhanced during the early stages of the anneals of as-grown material, but only by a small factor of ~ 3 . The feasibility of an explanation for such enhancements based on catalysis by atomic hydrogen was demonstrated by observation of much greater enhancements in material which had been subjected to a pretreatment in hydrogen gas.

There were apparent reductions in the rate, together with increases in the order of the $[\text{O}_i]$ -loss process, for anneals at higher temperatures ($T > 400^\circ\text{C}$). Despite these changes, no significant changes in the form of $[\text{O}_i]$ -loss data with increasing anneal time were observed. These observations could be explained by the increasing rate of dissociation of dimers present in a concentration that did not change significantly throughout the anneals. This quasiequilibrium could be achieved without the requirement of anomalously large values of D_{oxy} if O_2 dimers were assumed to diffuse much more rapidly than isolated O_i atoms. The $[\text{O}_i]$ -loss process can then be explained over the whole range of temperatures by varying the rates of dimer dissociation relative to dimer formation. The tendency to a dependence of $d[\text{O}_i]/dt$ on $[\text{O}_i]$ ⁸ in the case of anneals at the highest temperature (500°C) could then be explained if dimer clustering led predominantly to the formation or growth of large clusters, containing eight or more O atoms. Since the clusters formed by this mechanism can be the same over the whole temperature range, observations related to TD formation can be explained by associating TDs with different sizes of oxygen aggregates.

Note added in proof: The results presented here represent a significant update of the recently published review article of Newman and Jones.⁹⁰

ACKNOWLEDGMENTS

We thank Wackerchemitronic, Philips Components, and N. Sarno of MEMC Electronic Materials for supplying the material used in this work, and E. C. Lightowlers for help with the hydrogenation treatment; useful discussions with B. Pajot are gratefully acknowledged. The work was financially supported by the Science and Engineering Research Council (U.K.).

- ¹ P. D. Southgate, Proc. Phys. Soc. London **76**, 385 (1960).
- ² C. Haas, J. Phys. Chem. Solids **15**, 108 (1960).
- ³ J. W. Corbett, R. S. McDonald, and G. D. Watkins, J. Phys. Chem. Solids **25**, 873 (1964).
- ⁴ Y. Takano and M. Maki, in *Semiconductor Silicon*, edited by H. R. Huff and R. R. Burgess (Electrochemical Society, Princeton, NJ, 1973), p. 469.
- ⁵ J. Gass, H. H. Muller, H. Stüssi, and S. Schweiter, J. Appl. Phys. **51**, 2030 (1980).
- ⁶ J. C. Mikkelsen, Jr., Appl. Phys. Lett. **40**, 336 (1982).
- ⁷ M. Stavola, J. R. Patel, L. C. Kimerling, and P. E. Freeland, Appl. Phys. Lett. **42**, 73 (1983).
- ⁸ R. C. Newman, J. H. Tucker, and F. M. Livingston, J. Phys. C **16**, L151 (1983).
- ⁹ S.-T. Lee and D. Nichols, Appl. Phys. Lett. **47**, 1001 (1985).
- ¹⁰ R. C. Newman, A. S. Oates, and F. M. Livingston, J. Phys. C **16**, L667 (1983).
- ¹¹ R. C. Newman, J. Phys. C **18**, L967 (1985).
- ¹² W. Patrick, E. Hearn, W. Westdorp, and A. Bohg, J. Appl. Phys. **50**, 7156 (1979).
- ¹³ K. Wada and N. Inoue, J. Cryst. Growth **49**, 749 (1980).
- ¹⁴ K. Wada, H. Nakanishi, H. Takaoka, and N. Inoue, J. Cryst. Growth **57**, 535 (1982).
- ¹⁵ R. C. Newman, M. J. Binns, W. P. Brown, F. M. Livingston, S. Messoloras, R. J. Stewart, and J. G. Wilkes, Physica B **116**, 264 (1983).
- ¹⁶ F. M. Livingston, S. Messoloras, R. C. Newman, B. C. Pike, R. J. Stewart, M. J. Binns, W. P. Brown, and J. G. Wilkes, J. Phys. C **17**, 6253 (1984).
- ¹⁷ R. C. Newman, M. Claybourn, S. H. Kinder, S. Messoloras, A. S. Oates, and R. J. Stewart, in *Semiconductor Silicon*, edited by H. R. Huff, T. Abe, and B. Kolbesen (Electrochemical Society, Pennington, NJ, 1986), Vol. 86-4, p. 766.
- ¹⁸ F. S. Ham, J. Phys. Chem. Solids **6**, 335 (1958).
- ¹⁹ A. Ourmazd, W. Schröter, and A. Bourret, J. Appl. Phys. **56**, 1670 (1984).
- ²⁰ R. Bullough and R. C. Newman, Rep. Prog. Phys. **33**, 101 (1970).
- ²¹ U. M. Gösele, Mater. Res. Soc. Symp. **59**, 419 (1986).
- ²² T. Y. Tan, Mater. Res. Soc. Symp. **59**, 269 (1986).
- ²³ W. J. Taylor, T. Y. Tan, and U. M. Gösele, in *Defects in Silicon*, edited by W. M. Bullis, U. M. Gösele, and F. Shimura (Electrochemical Society, Pennington, NJ, 1991), p. 255.
- ²⁴ A. Bourret, J. Thibault-Desseaux, and D. N. Seidman, J. Appl. Phys. **55**, 825 (1984).
- ²⁵ H. Bender, Phys. Status Solidi A **86**, 245 (1984).
- ²⁶ W. Bergholz, J. L. Hutchison, and P. Pirouz, J. Appl. Phys. **58**, 3419 (1985).
- ²⁷ A. Bourret, Inst. Phys. Conf. Ser. **87**, 39 (1987).
- ²⁸ P. Pirouz, U. Dahman, K. H. Westmacott, and R. Chaim, Acta. Metall. Mater. **38**, 329 (1990).
- ²⁹ R. W. Carpenter, Y. L. Chen, M. J. Kim, and J. C. Barry, Inst. Phys. Conf. Ser. **100**, 543 (1989).
- ³⁰ R. C. Newman, in *20th International Conference on the Physics of Semiconductors*, edited by E. M. Anastassakis and J. D. Joannopoulos (World Scientific, Singapore, 1990), Vol. 1, p. 525.
- ³¹ S. Messoloras, R. C. Newman, R. J. Stewart, and J. H. Tucker, Semicond. Sci. Technol. **2**, 14 (1987).
- ³² S.-T. Lee and P. Fellingner, Appl. Phys. Lett. **49**, 1793 (1986).
- ³³ S.-T. Lee, P. Fellingner, and S. Chen, J. Appl. Phys. **63**, 1924 (1988).

- ³⁴D. Heck, R. E. Tressler, and J. Monkowski, *J. Appl. Phys.* **54**, 5739 (1983).
- ³⁵F. Shimura, T. Higuchi, and R. S. Hockett, *Appl. Phys. Lett.* **53**, 69 (1988).
- ³⁶L. Zhong and F. Shimura, *J. Appl. Phys.* **73**, 707 (1993).
- ³⁷W. Kaiser, H. L. Frisch, and H. Reiss, *Phys. Rev.* **112**, 1546 (1958).
- ³⁸D. Helmreich and E. Sirtl, in *Semiconductor Silicon*, edited by H. R. Huff, R. J. Kriegler, and Y. Takeishi (Electrochemical Society, Pennington, NJ, 1981), p. 626.
- ³⁹P. Gaworzewski and G. Ritter, *Phys. Status Solidi A* **67**, 511 (1981).
- ⁴⁰U. Gösele, K. Y. Ahn, B. P. R. Marioton, T. Y. Tan, and S.-T. Lee, *Appl. Phys. A* **48**, 219 (1989).
- ⁴¹C. A. Londos, M. J. Binns, A. R. Brown, S. A. McQuaid, and R. C. Newman, *Appl. Phys. Lett.* **62**, 1525 (1993).
- ⁴²T. Y. Tan, R. Kleinhenz, and C. P. Schneider, *Mater. Res. Soc. Symp. Proc.* **59**, 195 (1986).
- ⁴³R. C. Newman and M. Claybourn, *Inst. Phys. Conf. Ser.* **95**, 211 (1989).
- ⁴⁴A. R. Brown, R. Murray, R. C. Newman, and J. H. Tucker, *Mater. Res. Soc. Symp. Proc.* **163**, 555 (1990).
- ⁴⁵R. C. Newman, A. R. Brown, R. Murray, A. K. Tipping, and J. H. Tucker, in *Semiconductor Silicon*, edited by H. R. Huff, K. G. Barraclough, and J. Chikawa (Electrochemical Society, Pennington, NJ, 1990), Vol. 90-7, p. 734.
- ⁴⁶U. Gösele and T. Y. Tan, *Appl. Phys. A* **28**, 79 (1982).
- ⁴⁷L. C. Snyder, J. W. Corbett, P. Deák, and R. Wu, *Mater. Res. Soc. Symp. Proc.* **104**, 179 (1988).
- ⁴⁸M. Needels, J. D. Joannopoulos, Y. Bar-Yam, and S. T. Pantelides, *Phys. Rev. B* **43**, 4208 (1991).
- ⁴⁹P. Deák, L. C. Snyder, and J. W. Corbett, *Phys. Rev. B* **45**, 11 612 (1992).
- ⁵⁰R. Jones, *Semicond. Sci. Technol.* **5**, 255 (1990).
- ⁵¹S. A. McQuaid, R. C. Newman, J. H. Tucker, E. C. Lightowlers, R. A. A. Kubiak, and M. Goulding, *Appl. Phys. Lett.* **58**, 2933 (1991).
- ⁵²R. C. Newman, J. H. Tucker, and S. A. McQuaid, *Mater. Sci. Forum* **83-87**, 87 (1992).
- ⁵³*Standard Practices F120 for Determination of the Concentration of Impurities in Single Crystal Semiconductors Materials by Infrared Absorption Spectroscopy, Annual Book of ASTM Standards* (ASTM, Philadelphia, PA, 1987), Vol. 10.05.
- ⁵⁴A. Baghdadi, W. M. Bullis, M. C. Croarkin, L. Yue-zhen, R. I. Scace, R. W. Series, P. Stallhofer, and M. Watanabe, *J. Electrochem. Soc.* **36**, 2015 (1989).
- ⁵⁵A. Uhlir, *Bell Syst. Tech. J.* **34**, 105 (1955).
- ⁵⁶M. Claybourn and R. C. Newman, *Appl. Phys. Lett.* **52**, 2139 (1988).
- ⁵⁷A. R. Brown, M. Claybourn, R. Murray, P. S. Nandhra, R. C. Newman, and J. H. Tucker, *Semicond. Sci. Technol.* **3**, 591 (1988).
- ⁵⁸A. R. Brown, J. H. Tucker, R. C. Newman, and S. A. McQuaid, in *Proceedings of the 20th International Conference on the Physics of Semiconductors*, edited by E. M. Anastassakis and Joannopoulos (World Scientific, Singapore, 1990), Vol. 1, p. 553.
- ⁵⁹R. C. Newman, J. H. Tucker, A. R. Brown, and S. A. McQuaid, *J. Appl. Phys.* **70**, 3061 (1991).
- ⁶⁰S. A. McQuaid, M. J. Binns, R. C. Newman, E. C. Lightowlers, and J. B. Clegg, *Appl. Phys. Lett.* **62**, 1612 (1993).
- ⁶¹M. J. Binns, S. A. McQuaid, R. C. Newman, and E. C. Lightowlers, *Semicond. Sci. Technol.* **8**, 1908 (1993).
- ⁶²S. A. McQuaid, R. C. Newman, and E. C. Lightowlers, *Mater. Sci. Forum* **83-87**, 93 (1992).
- ⁶³I. A. Velorisoa, M. Stavola, D. M. Kozuch, R. E. Peale, and G. D. Watkins, *Appl. Phys. Lett.* **59**, 2121 (1991).
- ⁶⁴S. K. Estreicher, *Phys. Rev.* **41**, 9886 (1990).
- ⁶⁵R. Jones, S. Öberg, and A. Umerski, *Mater. Sci. Forum* **83-87**, 511 (1991).
- ⁶⁶A. K. Tipping, R. C. Newman, D. C. Newton, and J. H. Tucker, *Mater. Sci. Forum* **10-12**, 887 (1986).
- ⁶⁷W. Kern and D. Puotinen, *RCA Rev.* **31**, 187 (1970).
- ⁶⁸V. P. Markevich and L. I. Murin, *Phys. Status Solidi A* **111**, K149 (1989).
- ⁶⁹C. S. Fuller and R. A. Logan, *J. Appl. Phys.* **28**, 1427 (1957).
- ⁷⁰H. J. Stein and S. K. Hahn, *J. Appl. Phys.* **75**, 3477 (1994).
- ⁷¹E. C. Lightowlers, R. C. Newman, and J. H. Tucker, *Semicond. Sci. Technol.* **9**, 1370 (1994).
- ⁷²S. A. McQuaid, R. C. Newman, and E. C. Lightowlers, *Semicond. Sci. Technol.* **9**, 1736 (1994).
- ⁷³A. R. Bean and R. C. Newman, *J. Phys. Chem. Solids* **33**, 255 (1972).
- ⁷⁴M. J. Binns, Ph.D. thesis, University of London, 1993.
- ⁷⁵W. Kürner, R. Sauer, A. Dörnen, and K. Thonke, *Phys. Rev. B* **39**, 13 327 (1989).
- ⁷⁶P. J. Kelly, *Mater. Sci. Forum* **38-41**, 269 (1989).
- ⁷⁷A. R. Bean and R. C. Newman, *Solid State Commun.* **9**, 271 (1971).
- ⁷⁸A. S. Oates and R. C. Newman, *Appl. Phys. Lett.* **49**, 262 (1986).
- ⁷⁹J. L. Lindström and T. Hallberg, *Phys. Rev. Lett.* **72**, 2729 (1994).
- ⁸⁰J. Michel, J. R. Niklas, and J.-M. Spaeth, *Phys. Rev. B* **40**, 1732 (1989).
- ⁸¹T. Gregorkiewicz, H. H. P. Th. Bekman, and C. A. J. Amerlaan, *Phys. Rev. B* **41**, 12 628 (1990).
- ⁸²B. Pajot and J. von Bardeleben, in *Proceedings of the 13th International Conference on Defects in Semiconductors*, edited by L. C. Kimmerling and J. M. Parsey, Jr. (Metallurgical Society, Warrendale, PA, 1985), p. 685.
- ⁸³M. Claybourn and R. C. Newman, *Appl. Phys. Lett.* **51**, 2197 (1987).
- ⁸⁴V. P. Markevich, L. F. Makarenko, and L. I. Murin, *Phys. Status Solidi A* **97**, K173 (1986).
- ⁸⁵H. J. Stein, S. K. Hahn, and S. C. Shatas, *J. Appl. Phys.* **59**, 3495 (1986).
- ⁸⁶W. Götz, G. Pensl, and W. Zulehner, *Phys. Rev. B* **46**, 4312 (1992).
- ⁸⁷P. Wagner and J. Hage, *Appl. Phys. A* **49**, 123 (1989).
- ⁸⁸N. Meilwes, J.-M. Spaeth, V. V. Emtsev, G. A. Oganesyan, W. Götz, and G. Pensl, *Mater. Sci. Forum* **143-147**, 141 (1993).
- ⁸⁹M. Suezawa, in *Defects and Properties of Semiconductors: Defect Engineering*, edited by J. Chikawa, K. Sumino, and K. Wada (KTC, Tokyo, 1987), p. 219.
- ⁹⁰R. C. Newman and R. Jones, in *Semiconductors and Semimetals*, edited by F. Skimura (Academic, San Diego, CA, 1994), Vol. 42, Chap. 8, pp. 290-352.